

1 **Single cell transcriptomics reveals lineage trajectory of the retinal ganglion cells**  
2 **in wild-type and *Atoh7*-null retinas**

3  
4 Fuguo Wu<sup>1,2,\*</sup>, Jonathan E. Bard<sup>2,\*</sup>, Julien Kann<sup>2</sup>, Donald Yergeau<sup>2</sup>, Darshan Sapkota<sup>1,2</sup>,  
5 Yichen Ge<sup>1,2</sup>, Zihua Hu<sup>2</sup>, Jie Wang<sup>3</sup>, Tao Liu<sup>3</sup>, Xiuqian Mu<sup>1,2</sup>  
6

7 <sup>1</sup>Department of Ophthalmology/Ross Eye Institute, University at Buffalo, Buffalo, NY

8 <sup>2</sup>New York State Center of Excellence in Bioinformatics and Life Sciences, University at  
9 Buffalo, Buffalo, NY

10 <sup>3</sup>Department of Biostatistics & Bioinformatics, Roswell Park Comprehensive Cancer  
11 Center, Buffalo, NY

12

13 **Short title:** Developmental trajectory of the retinal ganglion cell lineage

14

15 **Corresponding author:** Xiuqian Mu, 701 Ellicott Street, Buffalo, NY, 14203. Tel: 001-  
16 716-881-7463; Fax: 001-716-849-6651; Email: [xmu@buffalo.edu](mailto:xmu@buffalo.edu)

17

18 \* These authors contributed equally to this project.

19

20 **Key Words:** Retinal development; Neural development; Transcription factors; Retinal  
21 ganglion cells; Gene regulation; bHLH transcription factors; Single cell RNA-seq

22

23

24 **Abstract:**

25 Past studies concluded that *Atoh7* is critical for the emergence of the retinal ganglion  
26 cell (RGC) lineage in the developing retina, whereas *Pou4f2* and *Isl1* function in RGC  
27 differentiation. *Atoh7* is expressed in a subset of retinal progenitor cells (RPCs) and is  
28 considered a competence factor for the RGC fate, but the molecular properties of these  
29 RPCs have not been well characterized. In this study, we first used conventional RNA-  
30 seq to investigate transcriptomic changes in *Atoh7*-, *Pou4f2*-, and *Isl1*-null retinas at  
31 embryonic (E) day 14.5 and identified the differentially expressed genes (DEGs), which  
32 expanded our understanding of the scope of downstream events. We then performed  
33 single cell RNA-seq (scRNA-seq) on E13.5 and E17.5 wild-type and *Atoh7*-null retinal  
34 cells. Clustering analysis not only correctly identified known cell types at these  
35 developmental stages but also revealed a transitional cell state which was marked by  
36 *Atoh7* and genes for other lineages in a highly overlapping fashion and shared by all  
37 early developmental trajectories. Further, analysis of the *Atoh7*-null retina revealed that,  
38 unlike previously believed, the RGC lineage still progressed considerably and a  
39 substantial amount of RGC-specific gene expression still occurred. Thus, *Atoh7* likely  
40 collaborates with other factors to shepherd the transitional RPCs to the RGC lineage by  
41 competing with other lineage factors and activating RGC-specific genes. This study thus  
42 provides significant insights into the nature of RPC competence for different retinal cell  
43 fates and revises our current view on the emergence of the RGC lineage.

44

## 45 Introduction

46 The central nervous system has the most diverse cellular composition in the animal  
47 body. How this complexity is achieved during development has been one of the central  
48 questions of neuroscience. In the central nervous system, all neural cell types originate  
49 from a common pool of neural progenitor cells; neural progenitor cells take on different  
50 developmental trajectories to eventually assume distinct cell fates. The neural retina is  
51 an ideal model for studying neural development. All retinal cell types arise from a single  
52 population of retinal progenitor cells (RPCs) through a conserved temporal sequence,  
53 but with significant overlaps<sup>1-4</sup>. The competence of RPCs for different cell fates change  
54 over the course of development so that different cell types are produced at different time  
55 windows<sup>4-12</sup>. Several factors influencing the temporal change of RPC competence have  
56 been identified<sup>13-16</sup>. However, multiple retinal cell types are often born in overlapping  
57 time windows, but the nature of RPC competence for individual cell types remains  
58 unknown. Based on gene expression, considerable heterogeneity has been observed  
59 within the general RPC population, which may be related to their competence for the  
60 various retinal cell fates<sup>17-24</sup>. In agreement with this idea, many key regulators, mostly  
61 transcription factors, expressed in subsets of RPCs have been shown to regulate  
62 different retinal cell fates<sup>21,21,23,25-30</sup>. Several RPC subpopulations including those  
63 expressing *Atoh7*, *Olig2*, *Neurog2*, and *Ascl1* are essential or biased for certain fates  
64<sup>17,19,31,32</sup>. However, the cell states in which these key transcription factors operate in, the  
65 actual complexity of RPC heterogeneity, the relationships between the different RPC  
66 sub-populations, and their relevance to RPC competence for individual retinal fates,  
67 have only begun to be addressed. Conventional experimental approaches have  
68 provided much insight into the genetic pathways and mechanisms underlying the  
69 formation of various retinal cell types<sup>1,33-35</sup>. However, the traditional approach of  
70 investigating individual genes and cell types has been painstakingly slow-paced and  
71 inefficient in providing a comprehensive picture, since the genesis of many cell types  
72 often occurs in overlapping time and space. Understanding the relationships among  
73 different progenitor subtypes and the progression of individual cell lineages is often  
74 limited by the knowledge of marker genes, the availability of proper reagents, and the  
75 low throughput and resolution and low qualitative nature of conventional multiplexing  
76 assays. Recent development in transcriptomics analysis using next-generation  
77 sequencing, particularly at single cell levels, affords powerful means to survey the  
78 complexity of cell composition and progression of cell states for individual cell lineages.

79 Single cell expression profiling (single cell RNA-seq, scRNA-seq) uses microfluidic  
80 devices to isolate single cells and generate barcoded cDNA libraries. The libraries are  
81 then sequenced by next-generation sequencing<sup>36,37</sup>. The sequence reads can then be  
82 decoded and attributed back to specific genes in individual cells, and expression levels  
83 of individual genes within each cell can then be determined. This approach enables the  
84 expression profiles of thousands of individual cells to be analyzed, and the cells can  
85 then be grouped (clustered) based on their similarities. The groups of cells thus  
86 identified from a developing tissue can reveal the cellular complexity of the tissue and  
87 the different cell states of individual cell lineages during development. The technology  
88 has been adopted to study many developing tissues and organs including the retina  
89<sup>13,36,38-45</sup>, and can thus be used to analyze the heterogeneity of RPCs and their

90 relationships to different retinal lineages. The current study focuses on one of the early  
91 retinal cell types, retinal ganglion cells (RGCs). Three key transcription factors, *Atoh7*,  
92 *Pou4f2*, and *Isl1*, function at different stages along the RGC lineage. *Atoh7* functions  
93 before the RGC fate is determined and is essential, but not sufficient, for the RGC fate  
94 <sup>22,25,30–32,46</sup>, whereas *Pou4f2* and *Isl1* function to specify the RGC fate and promote RGC  
95 differentiation <sup>47–51</sup>. *Atoh7* has thus been considered a competence factor. However,  
96 how the RGC lineage emerges in the global context of retinal development and what  
97 specific roles *Atoh7* plays in this process is not well understood.

98 To further understand RGC differentiation, we first performed conventional RNA-seq on  
99 mutant E14.5 retinas of the three key transcription factors genes, *Atoh7*, *Pou4f2*, and  
100 *Isl1*, to characterize the global downstream events during RGC development. This  
101 allowed us to expand the scope of downstream genes from previous studies and obtain  
102 a global view on the functions of these key regulators. We then performed scRNA-seq  
103 on retinal cells from E13.5 and E17.5 wild-type and *Atoh7*-null retinas. At these stages,  
104 particularly at E13.5, four major early retinal cell types, RGCs, horizontal cells, amacrine  
105 cells, and cones, are being generated <sup>4</sup>. Our analysis not only identified all these retinal  
106 cell types with unique gene signatures but also revealed their relationship to the RPC  
107 groups. Importantly, we discovered that all the early cell lineages went through a shared  
108 transitional cell state before the cell fates were committed and that this state was  
109 marked by such genes as *Atoh7*, *Neurog2*, *Neurod1*, and *Otx2* that are involved in the  
110 formation of these lineages. Analysis of the *Atoh7*-null cells revealed that the RGC  
111 trajectory was truncated as expected, with major changes in gene expression in  
112 individual cell types/states, particularly in RGCs. Unexpectedly, the RGC lineage still  
113 formed and advanced substantially, indicating that other factors are involved in  
114 establishing this lineage. These results provide novel insights into the mechanisms  
115 governing the emergence of the different retinal lineages and particularly advance our  
116 understanding of the cellular process and genetic pathways underlying the  
117 establishment of the RGC lineage.

## 118 **Material and methods**

### 119 Animals

120 All mice used were in the C57BL6/129 mixed genetic background. The two knockin  
121 alleles used in this study, *Atoh7*<sup>zsGreenCREERT2</sup> and *Pou4f2*<sup>FLAGtdTomato</sup>, were described in  
122 detail in a recent publication <sup>52</sup>. *Atoh7*<sup>zsGreenCREERT2</sup> is a null allele and *Pou4f2*<sup>FLAGtdTomato</sup>  
123 is a wild-type allele. The other alleles including *Atoh7*<sup>lacZ</sup> (null), *Pou4f2*<sup>Gfp</sup> (null), the  
124 conditional *Isl1*-null mice (*Isl1*<sup>flox/flox</sup>; *Six3-Cre*), and the *Atoh7*<sup>H1A</sup> allele were reported  
125 before <sup>18,30,49,53</sup>. All procedures using mice conform to the U.S. Public Health Service  
126 Policy on Humane Care and Use of Laboratory Animals and were approved by the  
127 Institutional Animal Care and Use Committees of Roswell Comprehensive Cancer  
128 Center and University at Buffalo.

### 129 Conventional RNA-seq



130 Conventional RNA-seq was carried out as previously described<sup>29</sup>. After timed mating,  
131 E14.5 retinas were dissected and stored in RNAlater (Invitrogen) while genotyping was  
132 performed. Three individual pools of four to six retinas were collected for individual  
133 genotypes, including wild-type, *Atoh7*-null (*Atoh7*<sup>lacZ/lacZ</sup>), *Pou4f2*-null (*Pou4f2*<sup>Gfp/Gfp</sup>), and  
134 *Isl1*-null (*Isl1*<sup>fllox/fllox</sup>; *Six3-Cre*). Total RNA was then isolated and RNA-seq libraries were  
135 generated using TruSeq RNA Sample Prep Kit v2 kit (Illumina, RS-122-2001) following  
136 the manufacturer's instruction and sequenced on an Illumina HiSeq2500 sequencer.  
137 Sequence reads were mapped to the mouse genome assembly (mm10) by STAR<sup>54</sup>  
138 and differentially expressed genes (DEGs) were identified by EdgeR<sup>55</sup>. The FDR cutoff  
139 was set at 0.05 and the minimum fold change imposed was 1.5. To compare gene  
140 expression changes in the three mutants, we calculated the z-scores of sequence read  
141 counts per million (CPM) for each gene, then divided the genes into five groups based  
142 on the hierarchical clustering. We then generated a heatmap of differential genes by the  
143 "pheatmap" R package (<https://cran.r-project.org/web/packages/pheatmap/index.html>).  
144 All RNA-seq sequence reads were deposited into the NCBI Short Read Archive  
145 (accession numbers SAMN02614558-SAMN02614569).

#### 146 Retinal cell dissociation, FACS, scRNA-seq library construction, and sequencing

147 Dissociation of embryonic retinas into single cell suspensions was performed as  
148 previously described<sup>56</sup>. E13.5 retinas with the desired genotypes were collected after  
149 timed mating. The genotypes used in this study included *Atoh7*<sup>zsGreenCreERT2/+</sup>  
150 (designated as wild-type) and *Atoh7*<sup>zsGreenCreERT2/lacZ</sup> (*Atoh7*-null). They were then  
151 washed with cold phosphate buffered solution, pH7.0 (PBS), and transferred to fresh  
152 tubes containing 200  $\mu$ l 10 mg/ml trypsin in PBS. The retinas were then incubated in a  
153 37°C water bath for 5 mins and triturated five times with a P1000 pipette tip. 20  $\mu$ l of  
154 soybean trypsin inhibitor was then added to the tube. The cells were spun down at 500  
155 g, washed twice with PBS, and resuspended in PBS. The cells were then loaded onto  
156 the 10X Genomics Chromium Controller to generate scRNA-seq libraries using the  
157 Chromium Single Cell 3' Library & Gel Bead Kit v2, following the manufacturer's  
158 instructions.

159 We also performed fluorescence assisted cell sorting (FACS) using relatively low gating  
160 thresholds as described to enrich *Atoh7*-expressing cells and *Pou4f2*-expressing cells  
161 from E17.5 retinas carrying the *Atoh7*<sup>zsGreenCreERT2</sup> and *Pou4f2*<sup>tdTomato</sup> alleles<sup>52</sup>. Cells  
162 from *Atoh7*<sup>zsGreenCreERT2/+</sup> and *Pou4f2*<sup>tdTomato/+</sup> were designated as wild-type, and those  
163 from *Atoh7*<sup>zsGreenCreERT2/lacZ</sup> were *Atoh7*-null. These cells were also loaded onto the 10X  
164 Genomics Chromium Controller to generate scRNA-seq libraries.

165 The libraries were sequenced by an Illumina HiSeq2500 rapid run using 26x8x98  
166 sequencing, and the reads were deposited into the NCBI Short Read Archive with a  
167 GEO accession number GSE149040.

#### 168 scRNA-Seq Analysis

169 The output from 10X Genomics Cellranger 2.1.1 pipeline was used as input into the R  
170 analysis package Seurat version 3.1.1. Cells with high unique molecular index counts  
171 (nUMI), high mitochondrial transcript load, and high transcript counts for red blood cell  
172 markers were filtered out from the analysis. The data was then r normalized, scaled,

173 and explored using Seurat's recommended workflow. Principal component analysis  
174 (PCA), Louvain clustering, and the UMAP (Uniform Manifold Approximation and  
175 Projection) were performed. Using the called clusters, cluster-to-cluster differential  
176 expression testing using the Wilcoxon Rank Sum identified unique gene markers for  
177 each cluster. Differential expression between shared wild-type and mutant clusters was  
178 assessed using the FindMarkers function of Seurat, which also utilized the Wilcoxon  
179 Rank Sum test. Cell cycle analysis used a protocol in Seurat with 70 cycle genes<sup>57</sup>  
180 ([https://satijalab.org/seurat/v3.1/cell\\_cycle\\_vignette.html](https://satijalab.org/seurat/v3.1/cell_cycle_vignette.html)).

181 To further interrogate the RGC developmental trajectory, cells belonging to C3, C4, C5,  
182 and C6 were subset from the Seurat data object. The average expression for each DEG,  
183 for each cluster, was compared between wildtype and *Atoh7*-null mice using the  
184 pheatmap package, clustering rows by euclidean distance using the hclust algorithm,  
185 and introducing cuts to the hierarchy tree using cutree = 7 for visual clarity.

### 186 Pseudotime Analysis

187 To infer developmental trajectories, the python package SCANPY provides  
188 pseudotemporal-ordering and the reconstruction of branching trajectories via Diffusion  
189 Pseudotime (DPT)<sup>58</sup>. A root cell was selected at random within the progenitor cell  
190 population of called Cluster 1. The assigned pseudotime values were then mapped  
191 back to the Seurat UMAP embedding for visualization and further analysis.

### 192 Immunofluorescence staining, In situ hybridization and online data mining

193 Immunofluorescence staining on cryopreserved retinal sections was performed as  
194 described before<sup>29,59</sup>. Primary antibodies used in this study included: rabbit anti-Otx2  
195 (1:200, Sigma, B74059), goat anti-Olig2 (1:200, R&D system, AF2418), mouse anti-  
196 Neurog2 (1:200, R&D system, MAB3314), goat anti-HA (1:100, Genscript, A00168),  
197 rabbit anti-Atoh7 (1:200, Novus, NBP1-88639), rabbit anti-Uchl1 (Pgp9.5) (1:500,  
198 Millipore, AB1761), mouse anti-Nefm (1:200, Sigma, N5264). Immunofluorescence  
199 images were captured by a Leica TCS SP2 confocal microscope. Positive cells were  
200 counted manually per arbitrary length unit as previously described<sup>29,56,59</sup>.

201 In situ hybridization was performed using RNAscope double Z probes (Advanced Cell  
202 Diagnostics) on paraffin-embedded retinal sections. After timed mating, embryos of  
203 desired stages were collected, fixed with 4% paraformaldehyde, embedded in paraffin,  
204 sectioned at 6  $\mu$ m, and de-waxed, as previously described<sup>29,49,59,60</sup>. The sections were  
205 then processed, hybridization was performed, and the signals were visualized using the  
206 RNAscope® 2.5 HD Detection Reagents-RED following the manufacturer's manual. In  
207 situ images were collected using a Nikon 80i Fluorescence Microscope equipped with a  
208 digital camera and Image Pro analysis software.

## 209 **Results**

### 210 **Changes in gene expression in *Atoh7*-, *Pou4f2*-, and *Isl1*-null retinas**

211 *Atoh7*, *Pou4f2*, and *Isl1* are three key regulators in the gene regulation network  
212 controlling RGC development<sup>49,59</sup>. They function at two different stages; *Atoh7* is  
213 believed to confer competence to RPCs for the RGC lineage, whereas *Pou4f2* and *Isl1*

214 function to specify the RGC fate and promote differentiation. Previously, downstream  
215 genes of *Atoh7*, *Pou4f2*, and *Isl1* have been identified by microarrays<sup>22,49,60,61</sup>. However,  
216 due to limitations of the technology used, those genes likely only cover small  
217 proportions of those regulated by the three transcription factors. To gain a more global  
218 view of the function of the three transcription factors, we collected total RNA samples  
219 from wild-type, *Atoh7*-null, *Pou4f2*-null, and *Isl1*-null retinal tissues at E14.5 and  
220 performed RNA-seq. The RNA-seq data from the wild-type retina provided a  
221 comprehensive list of genes expressed in the E14.5 retina with at least 1.0 average  
222 counts per million reads (CPM, see Suppl. Table 1). We then identified differentially  
223 expressed genes (DEGs) by edgeR<sup>55</sup> in each of these mutant retinas as compared to  
224 the wild-type retina using a cutoff of at least 1.5 fold change and FDR of at least 0.05  
225 (Suppl. Tables 2-4). In the *Atoh7*-null retina, we identified 670 downregulated genes  
226 including *Pou4f2* and *Isl1*, and 293 upregulated genes (Suppl. Table 2); in the *Pou4f2*-  
227 null retina, we identified 258 downregulated genes and 169 upregulated genes (Suppl.  
228 Table 3); and in the *Isl1*-null retina, we identified 129 downregulated genes and 79  
229 upregulated genes (Suppl. Table 4). Although *Atoh7* and *Pou4f2* were also identified as  
230 DEGs in their own respective mutant retinas, *Isl1* showed no change in the *Isl1*-null  
231 retina, because in the *Isl1*-null retina only the small frame-shifting exon 3 was deleted,  
232 which likely did not alter the mutant mRNA levels significantly<sup>49</sup>. These DEGs not only  
233 confirmed previous findings, as essentially all previously identified DEGs were included,  
234 but also provided a more complete picture by significantly increasing the numbers of  
235 DEGs for each mutant. The different numbers of DEGs in these three mutant retinas  
236 were consistent with their severity of defects in RGC development<sup>25,30,49,50,53</sup>, which  
237 was further reflected by a clustering heatmap analysis, showing that the *Atoh7*-null  
238 retina was least similar, and the *Isl1*-null retina was most similar, to the wild-type retina  
239 (Figure 1a).

240 Consistent with RGCs being largely missing in the *Atoh7*-null retina, RGC-specific  
241 genes were mostly found in the downregulated DEG list, whereas RPC-expressed  
242 DEGs included both down- and upregulated genes (Suppl. Table 2). The downregulated  
243 *Atoh7* gene list also encompassed the majority of genes in downregulated *Pou4f2* and  
244 *Isl1* lists, as would be expected considering that *Pou4f2* and *Isl1* function downstream of  
245 *Atoh7* (Figure 1b). Gene ontology (GO) analysis by DAVID<sup>62</sup> found the downregulated  
246 genes in the three mutants were highly associated with different aspects of neural  
247 differentiation, as demonstrated by enriched biological processes and GO terms,  
248 including nervous system development, axonogenesis, cell adhesion, and  
249 neurotransmitter secretion (Suppl. Table 5). On the other hand, the three upregulated  
250 gene lists were markedly different and much less overlapped (Figure 1c, Suppl. Tables  
251 2-4). GO analysis revealed the upregulated DEGs in the three mutants were broadly  
252 involved in neural development, both negatively and positively (Suppl. Table 5). Genes  
253 negatively regulating proliferation were enriched in the *Atoh7* upregulated list, but not  
254 the *Pou4f2* or *Isl1* upregulated list (Suppl. Table 5). These results reflected that these  
255 three factors repress gene expression largely independently at two different levels of the  
256 gene regulatory hierarchy either directly or indirectly; *Atoh7* represses gene expression  
257 in proliferating RPCs, confirming our previous analysis<sup>22</sup>, whereas *Pou4f2* and *Isl1*  
258 repress gene expression in RGCs. Independent gene repression by these factors was  
259 also demonstrated by genes with changes in different directions in these three mutant

260 retinas (Suppl. Tables 2-4). For example, *Nhlh1* did not change in *Atoh7*-null, was  
261 down-regulated in *Pou4f2*-null (fold change -2.2), but upregulated in *Isl1*-null (fold  
262 change 1.7), whereas its related gene *Nhlh2* was down-regulated (fold change -2.0) in  
263 *Atoh7*-null, did not change in *Pou4f2*-null, but was significantly up-regulated in *Isl1*-null  
264 (fold change 1.7). We also confirmed that some marker genes for amacrine cells (e.g.  
265 *Chat*, *Th*, fold change 383.0 and 35.1 respectively) were markedly up-regulated in  
266 *Pou4f2*-null as previously reported<sup>61</sup>, but they did not change in either *Atoh7*-null or  
267 *Isl1*-null retinas. *Dlx1* and *Dlx2*, two genes involved in RGC development<sup>63,64</sup>, were  
268 down-regulated in the *Atoh7*-null retina, but up-regulated in the *Pou4f2*- and *Isl1*-null  
269 retinas, indicating these genes were activated by *Atoh7* in RPCs, but repressed by  
270 *Pou4f2* and *Isl1* in RGCs (Suppl. Tables 2-4).

271 The DEG lists also revealed/confirmed that key pathways were affected in the three  
272 mutant retinas and additional components were found to be affected. For example, the  
273 Shh pathway, which is under the control of the gene regulatory network for RGC  
274 genesis, plays a key role in balancing proliferation and differentiation through a  
275 feedback mechanism<sup>49,50,60,65-68</sup>. Expanding previous findings, we found more  
276 components in the Shh pathway were affected in all three mutant retinas (Figure 2a,  
277 Suppl. Tables 2-4). These component genes, including *Shh*, *Gli1*, *Ptch1*, *Ptch2*, and  
278 *Hhip*, revealed a complex feedback loop of the pathway in balancing proliferation and  
279 differentiation via downstream genes such as *Gli1* and *CcnD1* (Cyclin D1) (Suppl.  
280 Tables 2-4, Figure 2b)<sup>49,50,60,65-71</sup>. Consistent with this model, expression of *Gli1* and  
281 *CcnD1* was reduced in all three mutants (Suppl. Tables 2-4). Two additional signaling  
282 pathways from RGCs to RPCs exist in the developing retina. Two related BMP  
283 molecules, *Gdf11* and *Myostatin/Gdf8* (*Mstn*), are also secreted from RGCs to balance  
284 RGC production and RPC proliferation<sup>60,72</sup>. *Vegf* is also involved in the feedback from  
285 RGCs to RPCs<sup>73</sup>. *Mstn* was downregulated in all three mutant retinas, but *Gdf11*  
286 exhibited no change, which may due to *Gdf11* expression not confined to just RGCs  
287 (data not shown). Unexpectedly, *Vegfa* expression increased in the *Atoh7*-null retina,  
288 although the underlying mechanism is not clear, but did not change in the other two  
289 mutants. Multiple component genes of the Notch pathway were upregulated in the  
290 *Atoh7*-null, but not the other two mutant retinas (Suppl. Tables 2-4). Some genes in the  
291 Notch pathway such as *Hes5* were also affected in the *Atoh7*-null retina (Suppl. Tables  
292 2). However, as discussed later with our single cell analysis, the effects of *Atoh7*  
293 deletion on the Notch pathway is complex and likely involved the Shh and *Vegf*  
294 pathways, as crosstalk exists between them via *Hes1*<sup>66,68,73,74</sup>. These results further  
295 demonstrated that deletion of *Atoh7* not only compromised RGC formation but also  
296 altered the properties of RPCs through multiple interacting pathways.

### 297 **Single cell RNA-seq of wild-type and *Atoh7*-null retinas at E13.5**

298 Whereas the RNA-seq data provided much insight into gene regulation by *Atoh7*,  
299 *Pou4f2*, and *Isl1* in the developing retina, how their absence affected different cell states  
300 could not be attained. Particularly for *Atoh7*, it functions in a subset of RPCs that gives  
301 rise to RGCs, but the properties of these RPCs and their relationships to other cell  
302 populations have not been well characterized. To that end, we first performed single cell  
303 RNA-seq with E13.5 wild-type and *Atoh7*-null retinal cells. The choice of E13.5, instead  
304 of E14.5, was fortuitous but did not affect our overall analysis since largely the same cell



305 types are being generated in these two time points <sup>2,4</sup>. After filtering out blood cells,  
306 doublet cells, and stressed cells, we were able to obtain expression data of 3521 wild-  
307 type cells and 6534 *Atoh7*-null cells. The median sequence reads were 68,491 and  
308 54,765 for wild-type and mutant cells respectively. The median numbers of genes  
309 captured were 1,975 and 2,375 for wild-type and mutant cells respectively. UMAP  
310 clustering was then performed on these cells using Seurat 3.1.1 <sup>75</sup>, which resulted in a  
311 total of 11 clusters (C0-C10) for both wild-type and *Atoh7*-null cells, and the  
312 corresponding clusters highly overlapped (Figure 3a, b). We first used known marker  
313 genes to assign identities to these clusters. These markers included *Ccnd1*, *Fgf15*, and  
314 *Sox2* for naïve RPCs <sup>24,65,76</sup>, *Sox2*, *Atoh7* and *Otx2* for subpopulations of RPCs <sup>18,23,77</sup>,  
315 *Pou4f2* and *Pou6f2* for RGCs <sup>78,79</sup>, *Ptf1a* and *Tfap2b* for amacrine and horizontal  
316 precursor cells <sup>27,28</sup>, *NeuroD4* and *Crx* for photoreceptors <sup>22,80,81</sup>, and *Otx1* and *Gja1* for  
317 ciliary margin cells <sup>82,83</sup>. At this stage, horizontal cells and amacrine cells seemed not to  
318 have fully diverged yet and thus were grouped together (Figure 3a, b). These marker  
319 genes were specifically expressed in distinct clusters as demonstrated by dot plots  
320 (Figure 3c) and feature plot heatmaps (Suppl. Figure 1). This allowed us to definitively  
321 designate their identities, including three clusters as naïve RPCs (C0-C2), two as  
322 transitional RPCs (C3 and C4) for reasons further discussed below, two as RGCs (C5  
323 and C6), one as horizontal and amacrine precursors (C7), two as photoreceptors (cones)  
324 (C8 and C9), and one as ciliary margin cells (C10). Notably and as expected, *Atoh7* was  
325 absent and the two RGC markers *Pou4f2* and *Pou6f2* were markedly diminished in the  
326 *Atoh7*-null cells, but the corresponding clusters in which they were expressed in the  
327 wild-type, including the two transitional RPC clusters (C3, C4) and two RGC clusters  
328 (C5, C6), still existed (Figure 3b, c, Suppl. Figure 1). Marker genes for the other mutant  
329 clusters did not show overt changes in their expression (Figure 3c, Suppl. Figure 1).  
330 These results were consistent with previous knowledge that RGCs, horizontal cells,  
331 amacrine cells, and cones are the major cell types being generated at this  
332 developmental stage <sup>2,4</sup>, and that deletion of *Atoh7* specifically affects RGCs <sup>25,30</sup>.

333 We also performed cell cycle analysis following a protocol in Seurat 3 using 70 cell  
334 cycle markers <sup>57</sup> and found that, for both wild-type and *Atoh7*-null cells, the three naïve  
335 progenitor cell clusters C0-C2 roughly co-segregated with their positions in the cell cycle,  
336 C0 in G1 and early S, C1 in S and G2/M, and C2 in G2/M (Figure 3d, e). The  
337 transitional RPCs (C3, C4) were also actively proliferating as they were found in  
338 different phases of the cell cycle, C3 in S and G2/M and C4 in G1. On the other hand,  
339 clusters composed of differentiating cells (C5, C6, C7, C8, C9) were all in G1 (G0)  
340 phase, confirming that they were indeed postmitotic neurons. These results  
341 demonstrated that our clustering analysis accurately grouped the cells into different  
342 stages of differentiation and our identity assignments were accurate.

### 343 **Relationships between the clusters**

344 To further examine the characteristics of the individual clusters, we performed gene  
345 enrichment analysis of the wild-type cells by comparing the expression profile of each  
346 cluster with those of all the other clusters and identified genes that were specifically  
347 enriched in individual clusters (Suppl. Table 6). The numbers of enriched genes in these  
348 clusters ranged from 126 to 686 with Cluster 6 having the most enriched genes (Suppl.  
349 Tables 6 and 7). The enriched genes further confirmed our initial cluster identity

350 assignment, as many additional known marker genes specific for the cell states/types  
351 were enriched in the corresponding clusters (Suppl. Table 6). Examples of such genes  
352 included *Sfrp2*, *Lhx2*, *Zfp3611*, and *Vsx2* for RPCs (C0-C2)<sup>14,84–86</sup>, *Isl1*, *Nefl*, *Sncg*,  
353 *Gap43*, and *Ina* for RGCs (C5 and C6)<sup>22,49,60</sup>, *Thrb*, *Meis2*, *Prdm1*, and *Gngt2* for  
354 photoreceptors (C8 and C9)<sup>87–90</sup>, *Tfap2a*, *Prdm13*, and *Onecut2* for amacrine and  
355 horizontal cell precursors (C7)<sup>29,91,92</sup>, and *Ccnd2* and *Msx1* for ciliary margin cells (C10)  
356 <sup>93,93,94</sup>.

357 Next, we examined the expression of the top ten enriched genes as ranked by p values  
358 from each wild-type cluster across all the clusters and represented the data by a  
359 heatmap (Figure 4a). This analysis did not only confirm their enrichment in the  
360 corresponding clusters but also revealed that many of these genes were expressed  
361 across several neighboring clusters, suggesting the relationships and continuity among  
362 these clusters along different developmental lineages. For example, the top ten  
363 enriched genes in C0 were also highly expressed in C1 and C2, indicating they indeed  
364 were all RPC clusters. The differences among these three clusters were likely due to  
365 their cell cycle status (Figure 3d), as many of the cluster-specific genes are directly  
366 involved in cell cycle regulation (Suppl. Table 6). C3 and C4 were two other examples of  
367 this continuity. They continued to express many of RPC genes enriched in C0-C2, albeit  
368 at lower levels, but began to express such genes as *Atoh7*, *Dlx1*, *Dlx2*, *Neurod1*, and  
369 *Otx2* which regulate retinal cell differentiation<sup>23,25,30,64,95</sup>. On the other hand, many of  
370 the genes in C3 and C4 trailed into the further differentiated clusters including C5 and  
371 C6 (RGCs), C7 (horizontal and amacrine cells), and C8 and C9 (photoreceptors),  
372 suggesting that C3 and C4 cells were intermediate transitional RPCs poised to  
373 differentiate (Figure 4a). Although C5 and C6 were both assigned as RGC clusters, C5  
374 continued to express many genes enriched in C3 and C4, but C6 essentially stopped  
375 expressing them (Figure 4a). On the other hand, although C5 cells expressed the early  
376 RGC marker genes such as *Isl1* and *Pou4f2* at high levels, they had not or had just  
377 begun to express many of the RGC-specific genes encoding RGC structure and  
378 function proteins such as *Nefl*, *Sncg*, *Gap43*, *Nefm*, and *Ina*, but these genes were  
379 highly expressed C6 cells (Figure 4a). Thus, C5 cells were nascent RGCs and C6 were  
380 further differentiated RGCs. Similarly, C8 were nascent photoreceptors and C9 were  
381 more differentiated photoreceptors based on the expression of early and later  
382 photoreceptor marker genes (Figure 4a). As mentioned above, C7 cells were  
383 considered precursors for horizontal and amacrine cells as they expressed genes  
384 required for both lineages such as *Ptf1a* but more specific marker genes for the two cell  
385 types were not robustly expressed yet. From these overlaps in expression the  
386 trajectories of the different cell lineages could be postulated, which all started from the  
387 naïve RPCs (C0-C2), underwent the transitional RPC stage (C3, C4), and finally  
388 reached the different terminal cell fates (C5-C9).

389 The unidirectional trajectories were further validated by examining the overlaps of all  
390 enriched gene lists in different clusters; there were significant overlaps between the  
391 naïve RPCs (C0-C2) and transitional RPCs (C3, C4), between the transitional RPCs  
392 (C3, C4) and the three terminal lineages including the RGC clusters C5 and C6,  
393 horizontal and amacrine cluster C7, photoreceptors clusters C8 and C9, but little  
394 overlaps between the naïve RPCs and fate-committed neurons (Figure 4b, and data not

395 shown), further confirming that C3 and C4 were in a transitional state linking naïve  
396 RPCs and differentiating neurons. Of note is that C10, which was composed of the  
397 ciliary margin cells with a unique gene signature, also expressed many of the genes  
398 enriched in RPC clusters C0-C2 (Figure 4a, Suppl Table 6), highlighting the close  
399 developmental relationship of the ciliary margin and the neural retina.

400 To further corroborate the relationships between the cells in these clusters, we also  
401 performed trajectory analysis using the SCANPY tool which is based on diffusion  
402 pseudotime (DPT) by measuring transitions between cells using diffusion-like random  
403 walks<sup>58</sup>. As shown in Figure 4c and consistent with the conclusions from the heatmap  
404 with the cluster-enriched genes, three definitive trajectories representing photoreceptors,  
405 horizontal and amacrine cells, and RGCs were identified, which all originated from the  
406 transitional RPCs that were downstream of the naïve RPC clusters. Not surprisingly,  
407 being the first cell types to form, the RGC trajectory advanced the furthest (Figure 4c).  
408 All three trajectories also existed in the *Atoh7*-null cells (Figure 4d); whereas the other  
409 two trajectories were not affected, the RGC trajectory appeared to have progressed  
410 through C5 but stalled at C6, consistent with the fact that RGCs are specifically affected  
411 in the *Atoh7*-null retina.

#### 412 **Characteristics of individual cell states during retinal development.**

413 To better understand the properties of the cell states/types represented by individual  
414 clusters, we further examined the biological function of the enriched genes in these  
415 clusters by GO analysis of each of these lists<sup>62</sup>. For simplicity, we combined similar  
416 clusters, including C0 to C2 (naïve RPCs), C3 and C4 (transitional RPCs), C5 and C6  
417 (RGCs), and C8 and C9 (photoreceptors) (Table 1). The top five GO biological  
418 processes enriched in naïve RPCs were cell cycle, cell division, mitotic nuclear division,  
419 nucleosome assembly, and chromosome segregation, confirming that they were indeed  
420 actively dividing RPCs at different phases of the cell cycle (Table 1). Two of the top five  
421 GO terms associated with C3 and C4 included cell cycle and cell division, further  
422 implying they were still RPCs. Interestingly, the other three top GO terms were all  
423 associated with RNA processing (Table 1), indicating that this process plays a critical  
424 role in these transitional RPCs. In contrast, GO terms enriched in RGCs, horizontal and  
425 amacrine cells, and photoreceptors were all related to the various aspect of neural  
426 development and function, further confirming that their identities were correctly assigned  
427 and that the enriched genes were involved in their formation.

428 The enriched gene lists also included many genes with unknown expression patterns  
429 and functions in the retina. To examine how faithful these enriched genes reflected their  
430 actual expression patterns in the developing retina, we chose genes from the enriched  
431 lists whose expression and function have not been well analyzed and compared their  
432 predicted expression patterns as presented by feature plots with that reported in the  
433 Eurexpress in situ hybridization database<sup>96</sup> (<http://www.eurexpress.org/ee/>). We found  
434 that the feature plots almost always correctly predicted the actual expression patterns,  
435 often with more details than in situ hybridization, as exemplified by 5 naïve RPC  
436 enriched genes and 10 RGC enriched genes whose expression and function in the  
437 retina have not been characterized (Suppl. Figures 2 and 3, Suppl. Table 6). Thus, the



438 clustering data based on scRNA-seq analysis can serve as a very useful resource for  
439 identifying novel genes as markers or candidates for further functional analysis.

440 The scRNA-seq data also clarified contradicting results on two genes critical in retinal  
441 development. *Sox4* and *Sox11*, which encodes two transcription factors critical for RGC  
442 development<sup>97-99</sup>, have been identified to be expressed mostly in RGCs, but there have  
443 been conflicting reports regarding whether they are also expressed in RPCs<sup>59,98-100</sup>. In  
444 the *Atoh7*-null retina, since most RGCs are absent, it was indicated that *Sox4* and  
445 *Sox11* were downregulated<sup>59,98</sup>. However, we did not detect significant changes in  
446 conventional RNA-seq analysis (Suppl. Table 2). These contradicting results were  
447 resolved by comparison of their expression in corresponding clusters; both genes were  
448 extensively expressed in all the clusters (Figure 5a, b), but were at lowest levels in  
449 naïve RPCs (C0-2), began to increase in the transitional RPCs (C3, C4), and reached  
450 the highest levels in RGCs (C5, C6) and amacrine and horizontal precursors (C7)  
451 (Figure 5c). These patterns were further confirmed by in situ hybridization with  
452 RNAscope probes<sup>101</sup> (Figure 5d, e). In the *Atoh7*-null retina, the overall patterns of  
453 *Sox4* and *Sox11* remained and the levels were comparable in all clusters, with only  
454 moderate upregulation of *Sox4* in differentiated RGCs (C6, Figure 5c). Therefore,  
455 despite the loss of RGCs, the overall expression levels of these two genes did not  
456 change in the *Atoh7*-null retina as detected by regular RNA-seq using total RNA from  
457 whole retinas. Nevertheless, as further discussed later, the differential expression levels  
458 of *Sox4* and *Sox11* along the differentiation trajectories may be related to their functions  
459 in the retina, particularly in RGC genesis.

#### 460 ***Atoh7* marks a transient state shared by all early differentiation cell fates**

461 Cells in C3 and C4 appeared to represent a critical transitional stage linking naïve RPCs  
462 and differentiating neurons along individual lineage trajectories. They were considered  
463 RPCs since they still were in the cell cycle (Figure 3d, e), expressed many RPC marker  
464 genes (Figure 4a, b, Suppl. Table 6), and their fate was not committed (Figure 4c).  
465 Nevertheless, expression of many of the general RPC marker genes was significantly  
466 decreased in these cells (Figures 3c, 4a). Close examination indicated that these cells  
467 expressed many genes involved in specific cell lineages, including *Atoh7*, *Sox4*, *Sox11*,  
468 *Neurog2*, *Neurod1*, *Otx2*, *Onecut1*, *Foxn4*, *Ascl1*, *Olig2*, *Dlx1*, *Dlx2*, and *Bhlhe22*  
469 (Figure 6a and Suppl. Table 6). These genes have all been reported to be expressed in  
470 subsets of RPCs, and function in or mark specific lineages. For example, *Atoh7* and  
471 *Neurog2* are required for the RGC lineage<sup>31,32,102</sup>, *Otx2* and *NeuroD1* function in the  
472 photoreceptor lineage<sup>23,95</sup>, whereas *Olig2*-expressing cells give rise to cone and  
473 horizontal progenies<sup>19</sup>. *Onecut1* and *Onecut2* function in essentially all the early retinal  
474 cell lineages<sup>26,29</sup>. Other such genes included *Foxn4* for horizontal and amacrine cells,  
475 *Dlx1* and *Dlx2* for RGCs and amacrine cells, and *Bhlhe22* (also known as *bHLHb5*) for  
476 amacrine cells and bipolar cells<sup>21,63,103-105</sup>.

477 The fact that these cells were clustered together and were enriched in these genes for  
478 different lineages indicated that they possessed shared properties. More interestingly,  
479 *Atoh7* was expressed in almost all cells in C3 (86%) and C4 (99%) and trailed into all  
480 three differentiating lineages (Figure 6a, b, c). Although this was consistent with  
481 previous findings that *Atoh7*-expressing cells are not fate-committed and can adopt all

482 retinal fates<sup>31,32,46</sup>, the high percentage of transitional RPCs expressing *Atoh7* was  
483 unexpected and likely significant. Moreover, several other factors such as *Neurog2*,  
484 *Neurod1*, and *Otx2* were also expressed in substantial portions of cells in C3 (68%,  
485 58%, and 38% respectively) and C4 (70%, 67%, and 66% respectively) (Figure 6a, b, c).  
486 Noticeably, in the *Atoh7*-null retina, the proportions of *Neurog2*- and *Neurod1*-  
487 expressing transitional RPCs (C3 and C4) only increased slightly, and that of *Otx2*-  
488 expressing transitional RPCs did not change (Figure 6c). *Neurog2* and *Neurod1* were  
489 essentially turned off in wild-type nascent RGCs (C5), but remained highly expressed in  
490 corresponding *Atoh7*-null cells (Figure 6c).

491 As the trajectories of individual lineages progressed, the relative activities of these  
492 genes changed accordingly. In the nascent RGCs (C5), whereas *Atoh7* continued to be  
493 expressed at high levels, *Neurog2*, *Neurod1*, and *Otx2* were much reduced in  
494 expression (Figure 6a, b, d). On the contrary, in the photoreceptor lineage (C8 and C9),  
495 *Atoh7* and *Neurog2* levels dropped significantly, but *Neurod1* and *Otx2* increased  
496 markedly (Figure 6a, b, d). As mentioned above, *Sox4* and *Sox11*, had elevated  
497 expression in the transitional RPCs (C3 and C4) and continued to be expressed in all  
498 lineages (Figures, 5a-c, 6a). Nevertheless, other factors, such as *Olig2*, *Onecut1*, *Foxn4*,  
499 *Ascl1*, seemed to be expressed in considerably fewer transitional RPCs (Figure 6a).  
500 However, the overlaps between these genes could be more extensive as the  
501 percentage of gene expression in each cluster was likely underestimated due to  
502 sequence depth and expression levels. Nevertheless, the transitional RPCs likely  
503 remained heterogeneous.

504 Another prominent feature of the transitional RPCs is that many genes encoding  
505 components of the Notch pathway, including *Dll1*, *Dll3*, *Dll4*, *Notch1*, *Hes5*, *Hes6*, and  
506 *Mfng* were enriched, further emphasizing the critical roles this pathway plays in retinal  
507 development (Figure 6e, Suppl. Table 6). The expression of *Dll1*, *Dll3*, and *Dll4* was of  
508 particular interest; they all were only expressed highly in transitional RPCs (C3 and C4)  
509 and the differentiating clusters, but not much in the naïve RPC clusters. Although *Hes5*,  
510 one of the effector genes of the pathway, was enriched, *Hes1*, another downstream  
511 effector of the pathway, was significantly downregulated in C3 and C4, as compared to  
512 the naïve RPCs (Suppl. Table 6 and data not shown), indicating that these two genes  
513 were differentially regulated and likely had both shared and distinct functions<sup>74,106</sup>.  
514 These findings suggested that when selected RPCs were poised for differentiation and  
515 began to express *Atoh7* and genes for other fates, they also elevated the levels of  
516 ligands of the Notch pathway, which in turn modulate the Notch activities in the naïve  
517 RPCs. Likely this is part of the mechanism by which the balance between proliferation  
518 and differentiation is achieved.

519 Many additional genes, e.g. *Gadd45a*, *Btg2*, *Penk*, *Srrm4*, and *Plk1*, *Sstr2*, and *Ccnb1*,  
520 were enriched in the transitional RPCs (Figure 6e, Suppl. Table 6), but their roles are  
521 mostly unknown. For example, *Gadd45a* and *Btg2*, two genes involved in cell cycle  
522 arrest, DNA repair and apoptosis<sup>107-110</sup>, were highly enriched in transitional RPCs, but  
523 they diverge in the differentiating lineages (Figure 6e). *Gadd45a* continued to be  
524 expressed in nascent RGCs (C5), whereas *Btg2* maintained its expression in  
525 photoreceptors (C8, C9) (Figure 6e). We further confirmed by RNAscope in situ  
526 hybridization that they each indeed were expressed in a subset of RPCs at different

527 developmental stages examined (E12.5, E14.5, and E17.5), with patterns very similar to  
528 that of *Atoh7*<sup>18,77,111</sup> (Suppl. Figure 4). Both genes are responsive to stress-induced  
529 growth arrest and inhibit the G1/S progression in the cell cycle. Although their roles in  
530 retinal development have not been well studied, they likely participate in establishing the  
531 transitional cell state in these cells, which are primed to exit the cell cycle and commit to  
532 distinct cell fates.

533 Our findings that *Atoh7* and genes for other cell lineages co-express in the transitional  
534 RPCs were consistent with previous co-immunofluorescence staining showing that  
535 *Atoh7* overlaps substantially with multiple relevant factors such as *Neurog2*, *Neurod1*,  
536 *Onecut1*, and *Onecut2*<sup>20,56,111</sup>. Further, by co-immunofluorescence staining, we  
537 confirmed that large proportions of *Olig2*-, *Otx2*- and *Foxn4*-expressing RPCs  
538 ( $67.53 \pm 4.66\%$ ,  $60.43 \pm 9.47$  and  $45.03 \pm 5.39$  respectively,  $n=4$ ) also expressed *Atoh7*  
539 (Figure. 6f-h). The relatively low percentage of *Foxn4* positive cells expressing *Atoh7*  
540 likely was due to *Foxn4* also being expressed in naïve RPCs (Figure 6a). These results  
541 indicated that all the early retinal cell fates go through a shared cell state which is  
542 characterized by downregulation of naïve RPC genes including those for cell cycle  
543 progression, upregulation of the Notch ligands, downregulation of the Notch pathway,  
544 and upregulation of neurogenic genes for various retinal fates. Of note is that, although  
545 *Atoh7* was expressed in essentially all transitional RPCs, deletion of *Atoh7* did not affect  
546 the formation of this cell state (Figures 3b, 6c), indicating that *Atoh7* is not required for  
547 the establishment of this critical cell state in retinal development.

#### 548 **Cell cluster-specific changes in gene expression in the *Atoh7*-null retina**

549 Corresponding E13.5 wild-type and *Atoh7*-null clusters almost completely overlapped in  
550 the 2D projection of the UMAP analysis (Figure 3a, b). Most clusters, including the  
551 transitional RPCs (C3 and C4), contained comparable proportions of cells in the wild-  
552 type and mutant retinas (Figure 7a). However, several clusters demonstrated marked  
553 changes. There was an about two-fold increase in the proportion of mutant C0 cells.  
554 Since most C0 cells were in G1/S of the cell cycle (Figure 2c, d), this may reflect the  
555 reduced proliferation of the naïve RPCs caused by reduced *Shh* signaling and the G1/S  
556 cyclin (*Cyclin D1*) levels (Figure 2)<sup>22,31,66,68,112</sup>, but the other pathways including the  
557 Notch pathway may also be involved. The cell number in mutant C7 reduced almost by  
558 half, which is consistent with previous reports suggesting that *Atoh7* plays a role in the  
559 genesis of horizontal cells<sup>31,59</sup>. There was also a noticeable drop in the number of  
560 nascent photoreceptor cells (C8), but no change in the more differentiated  
561 photoreceptors (C9). The significance of this observation is not known. The mutant  
562 cluster with the most significant change was C6, which were differentiating RGCs, with  
563 an ~5 fold reduction as compared to the wild-type cluster (Figure 7a). However, the  
564 nascent RGC cluster (C5) and the transitional RPC clusters (C3 and C4) did not show  
565 obvious changes in cell numbers. As discussed earlier, deletion of *Atoh7* did not  
566 substantially affect the overall cell cycle status of each cluster except for C0 as noted  
567 above, the relationships of the different clusters, or the overall trajectories of the distinct  
568 lineages (Figure 3a-e, Figure 4c, d).

569 The same corresponding clusters observed in the *Atoh7*-null retina provided us the  
570 opportunity to probe the cell state/type-specific gene expression changes caused by

571 deletion of *Atoh7*. Global gene expression between corresponding wild-type and *Atoh7*-  
572 null clusters were highly similar as revealed by the scatter plots; the correlation  
573 coefficients ( $R^2$ ) ranged from 0.870 to 0.969 (Figure 7b). The high  $R^2$  values indicated  
574 that gene expression levels detected by scRNA-seq were highly robust and  
575 reproducible. They were also consistent with the knowledge that *Atoh7* functions highly  
576 specifically in the RGC lineage. Accordingly, the two RGC clusters (C5 and C6) had the  
577 lowest  $R^2$  values (0.875 and 0.870 respectively). By comparing corresponding wild-type  
578 and *Atoh7*-null clusters, we identified a total of 1829 DEGs (Suppl. Tables 8-18).  
579 Comparison with the DEG list from conventional RNA-seq revealed an overlap of only  
580 290 genes (Suppl. Tables 2, 8-18). Further examination of the none-overlapped genes  
581 indicated scRNA-seq could not effectively detect DEGs with relatively low expression  
582 levels. For example, *Shh* was readily detected as a DEG by regular RNA-seq, but not  
583 by scRNA-seq, although *Gli1*, the downstream target gene of the Shh pathway, was  
584 detected by both methods (Figure 2a, Suppl. Tables 2, 8-10, 13, 14). This was likely  
585 due to the relatively low sequencing coverage of the transcriptome in scRNA-seq.  
586 Conventional RNA-seq, on the other hand, was inefficient in detecting DEGs that were  
587 expressed in multiple clusters but the change only occurred in selected clusters (see  
588 below). These results indicated that each method had limitations in identifying DEGs,  
589 particularly in tissues with complex cellular compositions, and that the two methods  
590 were complementary in providing a more complete picture of changes in gene  
591 expression.

592 Nevertheless, genes identified by comparing the corresponding wild-type and mutant  
593 clusters provided further insights into the function of *Atoh7*. Our focus will be on the  
594 DEGs in naïve RPCs (Suppl. Tables 8-10), transitional RPCs (Suppl. Tables 11, 12),  
595 and RGCs (Suppl. Tables 13, 14), since they were directly related to RGC development,  
596 whereas only small numbers of DEGs were detected for other clusters (Suppl. Tables  
597 15-18). Consistently, GO analysis of downregulated DEGs in naïve RPCs (C0-2) by  
598 DAVID revealed the top enriched biological process GO terms included protein folding,  
599 mRNA processing/RNA splicing, and cell division/cell cycle (Suppl. Table 8-10, 19).  
600 These biological processes are all required for active proliferation, which is a property of  
601 naïve RPCs. Example DEGs directly involved proliferation included *Ccnd1*, *Lig1*, *Mcm3*,  
602 and *Mcm7*. On the other hand, one of the prominent features of the biological processes  
603 associated with the upregulated DEGs is gene regulation associated with neural  
604 development (Suppl. Table 19). These results suggested that there was a shift in the  
605 properties of the naïve RPCs from proliferation to differentiation. Since *Atoh7* is not  
606 expressed in these cells (Figure 3c, Figure 6b), this shift likely was caused by non-cell  
607 autonomous mechanisms, highlighting the interaction between RGCs and RPCs. DEGs  
608 in the transitional RPCs (C3 and C4) likely reflected its direct function. Downregulated  
609 genes included those implicated in the RGC lineage such as *Dlx2* and *Eya2*, those  
610 involved in mRNA processing, and the Delta-like ligand genes (see below), but not cell  
611 cycle genes (Suppl. Tables 11, 12, 19). On the other hand, upregulated DEGs included  
612 those encoding a large number of transcription factors, many of which, such as *Foxn4*,  
613 *Neurod1*, and *Onecut2*, are involved in non-RGC lineages.

614 As expected, the largest number of DEGs were found between the wild-type and mutant  
615 RGC clusters (C5 and C6); 450 DEGs were found in C5, 618 DEGs were found in C6,



616 and collectively a total of 861 DEGs were identified in these two clusters (Suppl. Tables  
617 13, 14). These genes are directly relevant to the establishment and maintenance of the  
618 RGC identity; among them included *Pou4f2* and *Isl1* and many other previously  
619 identified genes encoding regulatory, functional, and structural proteins critical for RGC  
620 differentiation, which was further confirmed by GO analysis (Suppl. Table 19)<sup>49,50,59,60</sup>.  
621 As further discussed later, the upregulated DEGs in the mutant RGCs featured a large  
622 set of genes normally expressed in RPCs and/or other cell types including those of the  
623 Notch pathway (Suppl. Tables 13, 14). These upregulated DEGs indicated the RGC  
624 lineage, although still formed in the *Atoh7*-null retina, was immature and likely had  
625 mixed identities.

626 One interesting observation from the cluster-specific comparisons of the scRNA-seq  
627 data was that the Notch pathway was affected in a complex fashion in the *Atoh7*-null  
628 retina (Figure 7c, Suppl. Tables 8-17). In the naïve RPCs (C0-C2), *Hes1*, but not *Hes5*,  
629 was significantly down-regulated (Figure 7c, Suppl. Table 8-10), indicating the  
630 downregulation of the Notch pathway. Since *Hes1* is a convergent signaling node<sup>66,68,73</sup>,  
631 its downregulation likely resulted from the combined dysregulation of multiple pathways,  
632 including the Shh pathway, the Vegf pathway, and the Notch pathway its self.  
633 Consistently, in the transitional RPCs (C3 and C4), all three delta-like ligand genes, *Dll1*,  
634 *Dll3*, and *Dll4*, were markedly reduced, but other genes enriched in these cells,  
635 including *Notch1*, *Mfng*, and *Rbpj*, and *Hes6* did not change (Figure 7c, Suppl. Tables  
636 11, 12). On the other hand, multiple Notch pathway genes, including *Dll1*, *Dll3*, *Notch1*,  
637 *Mfng*, *Rbpj*, *Hes1*, and *Hes5*, were upregulated in RGCs (C5 and/or C6) (Figure 7c,  
638 Suppl. Tables 15, 16). Thus, *Atoh7*, which is expressed in the transitional RPCs, may  
639 influence the Notch pathway in multiple cell types, likely through regulating the Delta-  
640 like ligand genes directly and the other signaling pathways indirectly. As suggested  
641 above, the continued expression of Notch components in the RGCs may reflect their  
642 immaturity and stalled differentiation.

643 It is worth noting that the functions of many of the DEGs, both down- and upregulated,  
644 are unknown. Such examples included genes encoding members of the chaperonin  
645 containing TCP1 complex (*Cct3*, *Cct4*, *Cct5*, *Cct6A*, *Cct7*, *Cct8*), proteins involved in  
646 mRNA processing, and many transcription factors (e.g. *Insm1*, *Id1*, *Id2*, and *Id3*) (Suppl  
647 Tables 8-17). Further investigations are needed to understand their roles in the  
648 developing retina.

### 649 **The RGC lineage forms and advances substantially in the absence of *Atoh7***

650 The two clusters representing the RGC lineage (C5 and C6) were still present in the  
651 *Atoh7*-null retina (Figures 3b, Figure 7a). Although a significant reduction in cell number  
652 was found in more differentiated RGCs (C6) as expected, no major change in the  
653 proportion of nascent RGCs (C5) was observed in the *Atoh7*-null retina (Figure 7a).  
654 Thus, the RGC lineage was still formed initially, but its developmental trajectory staked  
655 prematurely (Figure 4c, d, Figure 7a). These findings indicated that, contrary to previous  
656 conclusions<sup>25,30</sup>, the RGC lineage still formed and advanced considerably in the  
657 absence of *Atoh7*, although most cells eventually failed to differentiate into fully  
658 functional RGCs.

659 To better understand the underlying genetic mechanisms for the defective RGC  
660 development in the *Atoh7*-null retina, we further examined the DEGs in C5 and C6 by  
661 comparing them (861 genes, Suppl. Table 13, 14) with the enriched genes in C5 and C6  
662 (821 genes, Suppl. Table 6), which were mostly RGC-specific genes (Figure 8a).  
663 Although a significant portion of the C5/C6 enriched genes (386 genes) were  
664 downregulated as expected, many of them did not change in expression (405 genes). A  
665 small number of C5/C6-enriched genes (34 genes) were upregulated. On the other  
666 hand, many downregulated DEGs (198 genes) and most upregulated DEGs (246 genes)  
667 were not enriched in C5/C6. These findings suggested these genes were regulated in  
668 different modes in the RGC lineage.

669 To further confirm these findings, we performed unsupervised clustering of all the 1266  
670 genes included in the C5/C6 DEG list and enriched gene list across the clusters of wild-  
671 type and *Atoh7*-null cells. This led to 7 groups of genes with distinct expression  
672 dynamics across the clusters, including RGC-enriched and downregulated (Group 1a,  
673 b); RGC-enriched but not significantly changed (Group 2); none RGC-enriched but  
674 upregulated (Group 3a, b); and none RGC-enriched but downregulated (Group 4a, b)  
675 (Figure 8b, only C3 to C6 are shown, and Suppl. Table 20). Example genes  
676 representing some of these distinct expression modes across different cell types/states  
677 were more clearly demonstrated by violin plots (Figure 8c). From these analyses, it was  
678 apparent that, as expected, a large proportion of RGC-specific genes, including *Pou4f2*,  
679 *Isl1*, *Syt4*, *Pou6f2*, *Gap43*, *Elavl4*, were downregulated in the *Atoh7*-null retina (Figure  
680 8). Among them, some genes such as *Pou4f2* and *Syt4* exhibited little expression in the  
681 mutant, but other genes, such as *Isl1* (data not shown), *Pou6f2*, *Gap43*, *Elavl4*, were  
682 still expressed at variable but substantial levels (Figure 8b, c). In addition, a substantial  
683 number of RGC genes such as *Nhlh2* remained expressed at similar levels as in the  
684 wild-type retina (Figure 8b, c). The remaining RGC-specific gene expression in the  
685 *Atoh7*-null retina, albeit often at lower levels, likely underlay the presence of nascent  
686 and differentiating RGCs.

687 Nevertheless, these RGCs not only failed to express a large number of genes either  
688 completely or at sufficient levels, but also aberrantly overexpressed many genes not  
689 enriched in RGCs (Groups 3a, b in Figure 8b, Figure 8c). Some of these genes, e.g.  
690 *Kctd8* (Figure 8c), were expressed at low levels in all wild-type clusters but were  
691 significantly upregulated specifically in RGCs (Group 3a). Other genes expressed in  
692 naïve and transitional RPCs but not in RGCs in the wild-type retina remained expressed  
693 in the mutant RGCs (Group 3b). As mentioned earlier, among these genes included the  
694 Notch pathway genes, *Neurod1*, and *Neurog2*. *Neurod1*, which is normally expressed in  
695 the transitional RPCs (C3 and C4) and photoreceptors (C8, and C9), but not in RGCs  
696 (C5 and C6) (Figure 6c,d, Figure 8c) became highly overexpressed in the *Atoh7*-null  
697 RGCs (Figure 8c).

698 The collective dysregulation of genes in *Atoh7*-null cells likely led to the truncated RGC  
699 trajectory. These cells progressed to an RGC-like state by expressing many of the RGC  
700 genes, often at reduced levels, but also overexpressed many genes abnormally.  
701 Because of the aberrant gene expression, they failed to fully differentiate into more  
702 mature RGCs and many of them, if not all, likely died<sup>32</sup>. Noticeably, in the *Atoh7*-null  
703 retina, we did not find increased expression of genes directly involved in apoptosis in

704 either the regular RNA-seq or scRNA-seq. This likely was due to the relatively small  
705 number of dying cells at any given time and that very few dying cells, if any, contributed  
706 to the single cell libraries.

### 707 **Effects on retinal development at E17.5 by *Atoh7* deletion**

708 To further investigate what occurred to the RGCs in the *Atoh7*-null retina as  
709 development proceeded, we also compared expression profiles of the wild-type and  
710 *Atoh7*-null retinas at E17.5, a time when RGC production significantly decreased<sup>4,18</sup>.  
711 Since the proportions of cells in RGC lineage become increasingly smaller as  
712 development advances<sup>4,18</sup>, we took advantage of two knockin-mouse lines,  
713 *Atoh7*<sup>zsGreenCreERT2</sup> and *Pou4f2*<sup>FlagtdTomato</sup>, which label *Atoh7*- and *Pou4f2*-expressing cells  
714 respectively, and enriched these cells by FACS<sup>52</sup>. Due to the stability of the zsGreen  
715 protein, zsGreen cells also included progenies of *Atoh7*-expressing cells, including  
716 RGCs, horizontal cells, and photoreceptors. We enriched *Atoh7*-expressing cells from  
717 both heterozygous (*Atoh7*<sup>zsGreenCreERT2/+</sup>, WT) and null retinas (*Atoh7*<sup>zsGreenCreERT2/lacZ</sup>,  
718 MT), as well as RGCs from the *Pou4f2*<sup>FlagtdTomato/+</sup> (WT) retina. We used low gating  
719 thresholds to enrich the relevant cell populations, but not to exclude other cell types,  
720 which allowed us to profile all the cell populations at E17.5 (see below). For simplicity of  
721 our analysis, zsGreen cells from the retina *Atoh7*<sup>zsGreenCreERT2</sup> and RGCs from the  
722 *Pou4f2*<sup>FlagtdTomato</sup> retina were grouped together (28,283 cells) as they are phenotypically  
723 wild-type, and compared with *Atoh7*-null cells (17,175 cells). As done with E13.5 cells,  
724 UMAP projection clustering and marker analysis allowed us to identify cell groups with  
725 similar cell identifies, including naïve RPCs, transitional RPCs, horizontal and amacrine  
726 cells, and photoreceptors for both wild-type and *Atoh7*-null cells, although the exact  
727 numbers of clusters differed and the identity of one cluster could not be ascertained  
728 (Figure 9, Suppl. Figure 5). Similar relationships from naïve RPCs to transitional RPCs,  
729 and then to fate-committed retinal cell types, were observed with both wild-type and  
730 *Atoh7*-null cells (Figure 9a). Importantly, transitional RPCs continued to express genes  
731 for multiple cell types with high overlaps, which included *Atoh7*, *Neurog2*, *NeuroD1*,  
732 *Otx2*, *Foxn4*, and *Olig2* (Figure 9b and data not shown). These genes, except *Atoh7*,  
733 were also expressed in the *Atoh7*-null transitional RPCs (Figure 9b and data not shown).  
734 The other genes expressed in the E13.5 transitional RPCs, including *Gadd45a* and *Btg2*,  
735 also continued to mark these cells at E17.5 (Suppl. Figure 5), indicating the general  
736 properties of these cells remained, although the cell types they produced had shifted.  
737 The presence of the RGC cluster in the E17.5 *Atoh7*-null retina suggested that some of  
738 the mutant RGCs persisted for some time. We further validated this by  
739 immunofluorescence staining for two RGC markers, *Nefm* and *Uchl1*, which showed  
740 that about 10-15% RGCs remained in the *Atoh7*-null retina at E17.5 (Suppl. Figure 6).

741 Comparison of the same clusters between wild-type and *Atoh7*-null retinas revealed the  
742 changes in E17.5 naïve RPCs largely followed the trend at E13.5 with many of the  
743 same genes affected in both stages (Suppl. Tables 21). For example, genes involved in  
744 cell cycle progression, including *Ccnd1*, *Mcm7*, *Mcm3*, and *Hes1*, continued to be  
745 downregulated, likely due to RGC loss and disrupted signaling from them. In the  
746 transitional RPCs, fewer genes were affected at smaller fold changes, likely reflecting  
747 the reduced activity of *Atoh7* and RGC production at this stage<sup>4,18,77</sup>, but many genes,  
748 such as *Dll3* and *Neurod1*, continued to be affected the same way as at E13.5 (Suppl.



749 Tables 22, 23). Consistently and unlike at E13.5, both wild-type and *Atoh7*-null RGC  
750 clusters were only tenuously connected to the transitional RPC clusters at E17.5 (Figure  
751 9a). In contrast to E13.5, there were only a small number of DEGs identified in the  
752 mutant RGCs at E17.5, and the fold changes tended to be smaller (Suppl. Table 24).  
753 However, these DEGs indicated that the remaining RGCs still were not normal.  
754 Whereas many RGC genes such as *Pou4f2*, *Elavl4*, *Nefm*, *Nefl* were expressed at the  
755 wild-type levels, other genes, e.g., *Crabp1*, *Gal*, *Sncg*, *Gap43*, *Ebf1*, *Ebf2*, *Ebf3*, *Klf7*,  
756 *Irx3*, *Irx5*, and *Isl1*, were downregulated. Intriguingly, *Pou6f2*, which was downregulated  
757 at E13.5 (fold change -2.9), was highly upregulated in the E17.5 *Atoh7*-null retina (fold  
758 change 2.5) (Figure 9c, Suppl Figure 6, Suppl. Tables 14, 24). Although the significance  
759 and mechanisms of the differential responses of the RGC genes in the *Atoh7*-null retina  
760 are unknown, they likely contributed to the eventual loss of almost all RGCs<sup>25,30</sup>.

## 761 Discussion

762 In this study, we first used regular RNA-seq to investigate the global transcriptomic  
763 changes in three mutant retinas, *Atoh7*-, *Pou4f2*-, and *Isl1*-null, during early  
764 development. The RNA-seq data provide a comprehensive list of genes expressed in  
765 the early developing retina (Suppl. Table 1). All genes known to function at this stage  
766 are on the list, and the gene list can be further mined for novel key regulators. Since all  
767 three mutants are defective in RGC development, this analysis provides a more  
768 complete picture and expands our knowledge of the function and hierarchical  
769 relationships of the three transcription factors in this lineage. The overlaps of  
770 downstream genes activated by the three factors confirm that *Atoh7* acts upstream,  
771 whereas *Pou4f2* and *Isl1* are dependent on *Atoh7* but only represent a part of the  
772 downstream events. Multiple signaling pathways are downstream of the three factors  
773 and functions through complex feedback mechanisms to coordinate proliferation and  
774 differentiation. Many RGC-specific genes were only dependent on *Atoh7*, but not on  
775 *Pou4f2* or *Isl1*, indicating other factors parallel to *Pou4f2* and *Isl1* are at work in the  
776 RGC lineage. On the other hand, the lists of upregulated genes, which are normally  
777 repressed by the three transcription factors, demonstrated that the three factors exert  
778 their repressive roles largely independently at two levels: *Atoh7* in RPCs whereas  
779 *Pou4f2* and *Isl1* in RGCs, although significant crosstalk between the two levels exists.

780 We then performed scRNA-seq on E13.5 and E17.5 wild-type and *Atoh7*-null retinal  
781 cells. The analysis not only correctly identified known cell states/types present at the  
782 stage, but also identified enriched genes for each cluster. The cluster-specific  
783 expression provided precise expression information not available before, demonstrating  
784 the power of this technology. Specifically, genes enriched in different clusters from our  
785 scRNA-seq data define specific states along the developmental trajectories and provide  
786 highly accurate information on their cell state/type-specific expression patterns (Figure  
787 10). These results not only validate several recent reports of scRNA-seq analysis of  
788 both mouse and human retinas showing the presence of distinct lineage trajectories and  
789 a shared transitional but plastic (multipotent) cell state (transitional RPCs) by all the  
790 early trajectories<sup>13,38,39,44</sup>, but also significantly extend those findings by revealing that  
791 *Atoh7* is expressed in all transitional RPCs and highly overlaps with genes involved in  
792 lineages other than RGCs. In agreement with our results, a similar finding that *Atoh7*  
793 marks transitional RPCs has also been reported with human embryonic retinal cells<sup>44</sup>.

794 Our study provides further insights into the nature of RPC competence for different  
795 retinal cell fates and the likely mechanism by which these fates are committed. Previous  
796 studies indicated that subsets of RPCs marked by specific genes exist and that these  
797 subsets are required for or biased toward particular cell fates<sup>17,19,31,32</sup>. However, the  
798 relationship between these RPC subpopulations and its relevance to the competence of  
799 RPCs for different retinal fates have not been known. Our current study establishes that  
800 these populations highly overlap and can be considered as a shared cell state of all  
801 early retinal cell types (Figure 10). This state is characterized by co-expression of genes  
802 essential for individual retinal cell types, such as *Atoh7* and *Neurog2* for RGCs, *Otx2*  
803 and *Neurod1* for photoreceptors, and *Foxn4* and *Onecut1/2* for amacrine and horizontal  
804 cells. The commonality of these factors is that they function before fate commitment but  
805 promote RPCs toward individual lineages. The transitional RPCs, still dividing but likely  
806 in the last cell cycle(s)<sup>18,31,32,46,111,112</sup>, are also characterized by significantly reduced  
807 expression of the naïve RPC markers and proliferation genes, increased expression of  
808 ligands for the Notch pathway, and decrease in the Notch pathway activities. These  
809 aspects of transition are likely coordinated, although the underlying mechanisms are not  
810 known. The Notch pathway is essential for RPC proliferation but inhibits differentiation  
811<sup>5,106,113,114,114–118</sup>. Promotion of proliferation by Notch may be achieved through  
812 interaction with some of the naïve RPC genes such as *Sox2*, *Lhx2*, and *Pax6*<sup>76,86,119,120</sup>.  
813 Consistently, retinal cell differentiation requires the downregulation of the Notch  
814 pathway<sup>5,115,121,122</sup>. Thus, downregulation of the Notch pathway likely is a key step for  
815 establishing this transitional state, and upregulation of the Notch ligands and other  
816 components may serve as a mechanism to balance proliferation and differentiation by  
817 lateral inhibition<sup>123–125</sup>. This downregulation is likely mediated in part by transcription  
818 factors like *Atoh7*, *Ascl1*, and *Foxn4*<sup>121,126,127</sup>. Our results indicate that *Atoh7* influences  
819 the Notch pathway in a complex fashion, both directly and indirectly, in different cell  
820 states/types. Additional genes, such as *Gadd45a*, *Btg2*, *Penk*, *Srrm4*, *Plk1*, *Sstr2*, and  
821 *Ccnb1*, were found highly expressed in this transitional state; they likely also play key  
822 roles in the transition from naïve RPCs to transitional RPCs.

823 Since all early cell types arise from these transitional RPCs, as suggested by our  
824 trajectory analysis, the long-postulated RPC competence for retinal cell fates may be  
825 determined and defined by the genes expressed in them. For example, their  
826 competence for the RGC fate is dictated at least in part by *Atoh7*, whose expression  
827 coincides with RGC production<sup>18,77,111</sup>. At later stages, when *Atoh7* is not expressed,  
828 RPCs lose their competence for the RGC fate. Consistent with the idea, deletion of  
829 *Atoh7* does not affect the establishment of this transitional state or the competences for  
830 other cell types. Since key regulators of different fates are co-expressed in these  
831 transitional RPCs, an outstanding question that arises is how the eventual outcome, i.e.  
832 adopting one particular fate versus another, is achieved. The mechanisms by which  
833 *Atoh7* promotes the RGC fate may serve as a point of discussion regarding how  
834 transitional RPCs take on a specific developmental trajectory. In agreement with  
835 previous findings that *Atoh7* is essential but not sufficient for the RGC lineage, we  
836 observed that *Atoh7* is expressed in all transitional RPCs and its expression trails into  
837 all three lineages being generated at E13.5. Since *Atoh7* is expressed in all transitional  
838 RPCs and thus significantly overlap with competent factors for other fates (e.g. *Neurod1*  
839 and *Otx2* for photoreceptors), these factors likely compete with each other to steer the

840 transitional RPCs toward different directions (Figure 10). The competition may occur at  
841 transcription levels through cross-repression as evidenced by the upregulation in the  
842 *Atoh7*-null retina of *Neurod1* and *Bhlhe22*, which are required for photoreceptors and  
843 amacrine cells respectively and by the distinct expression dynamics along different  
844 trajectories. However, this may not be the only or even the dominant mechanism, as  
845 other genes such as *Otx2* expressed in the transitional RPCs are not affected by the  
846 loss of *Atoh7*. Thus, *Atoh7* and the other competence factors may also compete with  
847 each other stochastically by activating distinct sets of downstream genes essential for  
848 the respective fates, e.g. *Pou4f2* and *Isl1* for the RGCs, *Ptf1a* for horizontal and  
849 amacrine cells, and *Crx* for photoreceptors. This idea is consistent with previous  
850 observations that RPCs generated different retinal cell types in a stochastic fashion<sup>7,8</sup>.  
851 Nevertheless, the eventual outcome is likely determined genetically; the proportion of  
852 different cell types produced at any given time is likely dictated by the presence of the  
853 competence factors and their relative activities. This idea is further supported by the  
854 finding that *Atoh7* gene dosage affects the number of RGCs produced and that  
855 overexpression of *Atoh7* produces more RGCs<sup>128–130</sup>. Activities of these transcription  
856 factors may also be modified posttranslationally<sup>131–134</sup>. On the other hand, the  
857 transitional RPCs are still heterogeneous, as indicated by the uneven expression of  
858 many genes in these cells. This has also been demonstrated by lineage-tracing  
859 experiments; although *Olig2*, *Neurog2*, and *Ascl1* are all expressed in transitional RPCs,  
860 cells expressing these genes are biased in producing specific retinal progenies<sup>17,19</sup>.  
861 The heterogeneity of transitional RPCs may reflect their different degree of progression  
862 toward different developmental trajectories.

863 Our scRNA-seq analysis on the *Atoh7*-null retina leads to significant insights into RGC  
864 development by identifying specific changes in gene expression through both direct and  
865 indirect mechanisms. Of particular significance was our observation that in the absence  
866 of *Atoh7*, the RGC trajectory still progressed considerably, but stalked prematurely. This  
867 may have been observed previously but not fully appreciated; many of the mutant  
868 *Atoh7*-expressing cells, marked by knock-in lacZ or Cre-activated reporter markers, still  
869 migrate to the inner side where RGCs normally reside<sup>25,30,31,46</sup>, but many of them likely  
870 die by apoptosis<sup>32</sup>, although some of these cells may redirect and adopt other fates.  
871 However, the status of these cells has not been well characterized. Our results indicate  
872 that these cells are on the RGC trajectory, and many, but not all, RGC-specific genes  
873 are activated in them, although often not to the wild-type levels. Some of the mutant  
874 RGCs even persist for some time but still have aberrant gene expression. Consistent  
875 with our findings, when apoptosis is inhibited, a much larger number of RGCs survived  
876<sup>135</sup>. These new findings suggest that additional factor(s) other than *Atoh7* function in the  
877 transitional RPCs to promote them toward the RGC lineage. Whereas *Neurod1* and  
878 *Neurog2*, which are upregulated in the *Atoh7*-null retina, may be compensatory, they  
879 unlikely play major roles in the RGC lineage, as mutations of their genes lead to  
880 relatively minor RGC defects<sup>20,102,136</sup>. We propose that the SoxC family of transcription  
881 factors, including Sox4 and Sox11, fulfill this role (Figure 10). This is based on previous  
882 reports that deletion of the SoxC genes leads to severely compromised RGC production  
883<sup>97–99</sup>, and our finding that they are expressed at high levels in the transitional RPCs and  
884 that their expression is not dependent on *Atoh7*. The SoxC factors likely also function in  
885 differentiating RGCs and other cell types, as they continue to be expressed in fate-

886 committed retinal neurons. Thus, activation of early RGC genes such as *Pou4f2* and  
887 *Isl1*, likely requires both upstream inputs, but in the absence of *Atoh7*, the SoxC factors  
888 still activate some of the RGC genes (Figure 10). Ectopic expression of *Pou4f2* and *Isl1*  
889 together rescues RGC formation caused by deletion of *Atoh7*, and the two factors were  
890 proposed to be part of a core group of factors determining the RGC fate<sup>59</sup>. In light of  
891 our current findings, the determination of the RGC fate is likely a gradual process over a  
892 time window without a clear boundary, and the function of *Pou4f2* and *Isl1* is to stabilize  
893 the developmental trajectory by activating genes essential for RGC differentiation and  
894 repressing genes for other fates. Some of the RGC genes are activated already by  
895 *Atoh7* and/or other factors independent of *Pou4f2* and *Isl1*, but require *Pou4f2* and *Isl1*  
896 to reach full amplitudes of expression, whereas many other RGC genes can only be  
897 activated by *Pou4f2* and *Isl1* (Figure 10). Other than activating RGC genes, *Atoh7* is  
898 also involved in other aspects of RGC genesis, such as cell cycle exit, downregulation  
899 of the Notch pathway, and even generation of other cell types<sup>32,39,130</sup>. Elucidating the  
900 full function of *Atoh7* requires identification of its direct targets and the associated  
901 epigenetic status.

902 Our study also demonstrates that regular RNA-seq and scRNA-seq complement each  
903 other and can be used in combination to provide much richer information regarding  
904 transcriptomic changes due to genetic perturbations. Although regular RNA-seq lacks  
905 cellular resolution, it is more sensitive in detecting genes expressed at low levels and/or  
906 in a smaller number of cells. On the other hand, scRNA-seq enables classification of  
907 cell states/types in complex tissues and provides insights into relationships among the  
908 different cell states/types. scRNA-seq also provides precise information regarding  
909 changes in gene expression in specific cell states/types. It is worth noting that, currently,  
910 likely due to limitations of sequence depth and library construction, genes expressed at  
911 low levels and/or in small numbers of cells are not always readily detectable by scRNA-  
912 seq, but this may change as the technology further matures.

913 In summary, we used RNA-seq and scRNA-seq to survey gene expression in the  
914 developing retina and identify changes associated with deletion of key transcription  
915 factor genes for the RGC lineage. Our results provide a global view of the gene  
916 expression, cell states, and their relationships in early retinal development. Furthermore,  
917 our study validates and further defines a transitional state shared by all early retinal cell  
918 fates (Figure 10). *Atoh7*, likely in collaboration with other factors, functions within this  
919 cell state to shepherd RPCs to the RGC lineage by competing with other lineage factors  
920 and activating RGC-specific genes. Further analysis of the shifts in the epigenetic  
921 landscape along individual trajectories in both wild-type and mutant retinas will help  
922 elucidate the underlying mechanisms of RGC differentiation.

## 923 **Acknowledgments**

924 We thank other members of the Mu laboratory and members of the Department of  
925 Ophthalmology and the Developmental Genomics Group, University of Buffalo, for  
926 helpful discussions. We also would like to thank Andrew Kelly for technical support. The  
927 knockin mouse lines were created by the Gene Targeting and Transgenic Resource  
928 Core at the Roswell Park Cancer Institute. Construction and sequencing of RNA-seq  
929 and scRNA-seq libraries were carried out at the Genomics and Bioinformatics Core of

930 University at Buffalo. This project was supported by grants from the BrightFocus  
931 Foundation (G2016024) and the National Eye Institute of the National Institutes of  
932 Health (R01EY020545 and R01EY029705) to X.M. The content is solely the  
933 responsibility of the authors and does not necessarily represent the official views of the  
934 National Institutes of Health.



935 **References:**

- 936 1. Cepko, C. Intrinsically different retinal progenitor cells produce specific types of  
937 progeny. *Nat Rev Neurosci* **15**, 615–27 (2014).
- 938 2. Cepko, C. L., Austin, C. P., Yang, X., Alexiades, M. & Ezzeddine, D. Cell fate  
939 determination in the vertebrate retina. *Proc Natl Acad Sci U S A* **93**, 589–95 (1996).
- 940 3. Livesey, F. J. & Cepko, C. L. Vertebrate neural cell-fate determination: lessons  
941 from the retina. *Nat Rev Neurosci* **2**, 109–18 (2001).
- 942 4. Young, R. W. Cell differentiation in the retina of the mouse. *Anat Rec* **212**, 199–205  
943 (1985).
- 944 5. Austin, C. P., Feldman, D. E., Ida, J. A., Jr. & Cepko, C. L. Vertebrate retinal  
945 ganglion cells are selected from competent progenitors by the action of Notch.  
946 *Development* **121**, 3637–50 (1995).
- 947 6. Belecky-Adams, T., Cook, B. & Adler, R. Correlations between terminal mitosis and  
948 differentiated fate of retinal precursor cells in vivo and in vitro: analysis with the  
949 ‘window-labeling’ technique. *Dev Biol* **178**, 304–15 (1996).
- 950 7. Cayouette, M., Barres, B. A. & Raff, M. Importance of intrinsic mechanisms in cell  
951 fate decisions in the developing rat retina. *Neuron* **40**, 897–904 (2003).
- 952 8. Gomes, F. L. *et al.* Reconstruction of rat retinal progenitor cell lineages in vitro  
953 reveals a surprising degree of stochasticity in cell fate decisions. *Development* **138**,  
954 227–35 (2011).
- 955 9. La Vail, M. M., Rapaport, D. H. & Rakic, P. Cytogenesis in the monkey retina. *J*  
956 *Comp Neurol* **309**, 86–114 (1991).
- 957 10. Rapaport, D. H., Wong, L. L., Wood, E. D., Yasumura, D. & LaVail, M. M. Timing  
958 and topography of cell genesis in the rat retina. *J Comp Neurol* **474**, 304–24 (2004).
- 959 11. Reh, T. A. & Kljavin, I. J. Age of differentiation determines rat retinal germinal cell  
960 phenotype: induction of differentiation by dissociation. *J Neurosci* **9**, 4179–89  
961 (1989).
- 962 12. Wong, L. L. & Rapaport, D. H. Defining retinal progenitor cell competence in  
963 *Xenopus laevis* by clonal analysis. *Development* **136**, 1707–15 (2009).
- 964 13. Clark, B. S. *et al.* Single-Cell RNA-Seq Analysis of Retinal Development Identifies  
965 NFI Factors as Regulating Mitotic Exit and Late-Born Cell Specification. *Neuron*  
966 **102**, 1111–1126 (2019).
- 967 14. Gordon, P. J. *et al.* Lhx2 balances progenitor maintenance with neurogenic output  
968 and promotes competence state progression in the developing retina. *J Neurosci*  
969 **33**, 12197–207 (2013).
- 970 15. La Torre, A., Georgi, S. & Reh, T. A. Conserved microRNA pathway regulates  
971 developmental timing of retinal neurogenesis. *Proc Natl Acad Sci U S A* **110**, E2362-  
972 70 (2013).
- 973 16. Mattar, P., Ericson, J., Blackshaw, S. & Cayouette, M. A conserved regulatory logic  
974 controls temporal identity in mouse neural progenitors. *Neuron* **85**, 497–504 (2015).
- 975 17. Brzezinski, J. A. th, Kim, E. J., Johnson, J. E. & Reh, T. A. Ascl1 expression  
976 defines a subpopulation of lineage-restricted progenitors in the mammalian retina.  
977 *Development* **138**, 3519–31 (2011).
- 978 18. Fu, X. *et al.* Epitope-tagging Math5 and Pou4f2: new tools to study retinal ganglion  
979 cell development in the mouse. *Dev Dyn* **238**, 2309–17 (2009).

- 980 19. Hafler, B. P. *et al.* Transcription factor Olig2 defines subpopulations of retinal  
981 progenitor cells biased toward specific cell fates. *Proc Natl Acad Sci U A* **109**,  
982 7882–7 (2012).
- 983 20. Kiyama, T. *et al.* Overlapping spatiotemporal patterns of regulatory gene  
984 expression are required for neuronal progenitors to specify retinal ganglion cell fate.  
985 *Vis. Res* **51**, 251–9 (2011).
- 986 21. Li, S. *et al.* Foxn4 controls the genesis of amacrine and horizontal cells by retinal  
987 progenitors. *Neuron* **43**, 795–807 (2004).
- 988 22. Mu, X. *et al.* A gene network downstream of transcription factor Math5 regulates  
989 retinal progenitor cell competence and ganglion cell fate. *Dev Biol* **280**, 467–81  
990 (2005).
- 991 23. Nishida, A. *et al.* Otx2 homeobox gene controls retinal photoreceptor cell fate and  
992 pineal gland development. *Nat Neurosci* **6**, 1255–63 (2003).
- 993 24. Trimarchi, J. M., Stadler, M. B. & Cepko, C. L. Individual retinal progenitor cells  
994 display extensive heterogeneity of gene expression. *PLoS One* **3**, e1588 (2008).
- 995 25. Brown, N. L., Patel, S., Brzezinski, J. & Glaser, T. Math5 is required for retinal  
996 ganglion cell and optic nerve formation. *Development* **128**, 2497–508 (2001).
- 997 26. Emerson, M. M., Surzenko, N., Goetz, J. J., Trimarchi, J. & Cepko, C. L. Otx2 and  
998 *Onecut1* promote the fates of cone photoreceptors and horizontal cells and repress  
999 rod photoreceptors. *Dev Cell* **26**, 59–72 (2013).
- 1000 27. Fujitani, Y. *et al.* Ptf1a determines horizontal and amacrine cell fates during mouse  
1001 retinal development. *Development* **133**, 4439–50 (2006).
- 1002 28. Nakhai, H. *et al.* Ptf1a is essential for the differentiation of GABAergic and  
1003 glycinergic amacrine cells and horizontal cells in the mouse retina. *Development*  
1004 **134**, 1151–60 (2007).
- 1005 29. Sapkota, D. *et al.* *Onecut1* and *Onecut2* redundantly regulate early retinal cell fates  
1006 during development. *Proc Natl Acad Sci U A* **111**, E4086–4095 (2014).
- 1007 30. Wang, S. W. *et al.* Requirement for *math5* in the development of retinal ganglion  
1008 cells. *Genes Dev* **15**, 24–9 (2001).
- 1009 31. Brzezinski, J. A. th, Prasov, L. & Glaser, T. Math5 defines the ganglion cell  
1010 competence state in a subpopulation of retinal progenitor cells exiting the cell cycle.  
1011 *Dev Biol* **365**, 395–413 (2012).
- 1012 32. Feng, L. *et al.* MATH5 controls the acquisition of multiple retinal cell fates. *Mol*  
1013 *Brain* **3**, 36 (2010).
- 1014 33. Bassett, E. A. & Wallace, V. A. Cell fate determination in the vertebrate retina.  
1015 *Trends Neurosci* **35**, 565–73 (2012).
- 1016 34. Swaroop, A., Kim, D. & Forrest, D. Transcriptional regulation of photoreceptor  
1017 development and homeostasis in the mammalian retina. *Nat Rev Neurosci* **11**,  
1018 563–76 (2010).
- 1019 35. Xiang, M. Intrinsic control of mammalian retinogenesis. *Cell Mol Life Sci* **70**, 2519–  
1020 32 (2013).
- 1021 36. Macosko, E. Z. *et al.* Highly Parallel Genome-wide Expression Profiling of  
1022 Individual Cells Using Nanoliter Droplets. *Cell* **161**, 1202–1214 (2015).
- 1023 37. Zheng, G. X. Y. *et al.* Massively parallel digital transcriptional profiling of single  
1024 cells. *Nat. Commun.* **8**, 1–12 (2017).



- 1025 38. Giudice, Q. L., Leleu, M., Manno, G. L. & Fabre, P. J. Single-cell transcriptional  
1026 logic of cell-fate specification and axon guidance in early-born retinal neurons.  
1027 *Development* **146**, dev178103 (2019).
- 1028 39. Lu, Y. *et al.* Single-Cell Analysis of Human Retina Identifies Evolutionarily  
1029 Conserved and Species-Specific Mechanisms Controlling Development. *Dev. Cell*  
1030 (2020) doi:10.1016/j.devcel.2020.04.009.
- 1031 40. Lukowski, S. W. *et al.* A single-cell transcriptome atlas of the adult human retina.  
1032 *EMBO J.* e100811 (2019) doi:10.15252/embj.2018100811.
- 1033 41. Menon, M. *et al.* Single-cell transcriptomic atlas of the human retina identifies cell  
1034 types associated with age-related macular degeneration. *Nat. Commun.* **10**, 1–9  
1035 (2019).
- 1036 42. Rheaume, B. A. *et al.* Single cell transcriptome profiling of retinal ganglion cells  
1037 identifies cellular subtypes. *Nat. Commun.* **9**, 2759 (2018).
- 1038 43. Shekhar, K. *et al.* Comprehensive Classification of Retinal Bipolar Neurons by  
1039 Single-Cell Transcriptomics. *Cell* **166**, 1308–1323 (2016).
- 1040 44. Sridhar, A. *et al.* Single-Cell Transcriptomic Comparison of Human Fetal Retina,  
1041 hPSC-Derived Retinal Organoids, and Long-Term Retinal Cultures. *Cell Rep.* **30**,  
1042 1644-1659.e4 (2020).
- 1043 45. Tran, N. M. *et al.* Single-Cell Profiles of Retinal Ganglion Cells Differing in  
1044 Resilience to Injury Reveal Neuroprotective Genes. *Neuron* **104**, 1039-1055.e12  
1045 (2019).
- 1046 46. Yang, Z., Ding, K., Pan, L., Deng, M. & Gan, L. Math5 determines the competence  
1047 state of retinal ganglion cell progenitors. *Dev Biol* **264**, 240–54 (2003).
- 1048 47. Erkman, L. *et al.* Role of transcription factors Brn-3.1 and Brn-3.2 in auditory and  
1049 visual system development. *Nature* **381**, 603–6 (1996).
- 1050 48. Gan, L. *et al.* POU domain factor Brn-3b is required for the development of a large  
1051 set of retinal ganglion cells. *Proc Natl Acad Sci U S A* **93**, 3920–5 (1996).
- 1052 49. Mu, X., Fu, X., Beremand, P. D., Thomas, T. L. & Klein, W. H. Gene regulation  
1053 logic in retinal ganglion cell development: Isl1 defines a critical branch distinct from  
1054 but overlapping with Pou4f2. *Proc Natl Acad Sci U S A* **105**, 6942–7 (2008).
- 1055 50. Pan, L., Deng, M., Xie, X. & Gan, L. ISL1 and BRN3B co-regulate the  
1056 differentiation of murine retinal ganglion cells. *Development* **135**, 1981–90 (2008).
- 1057 51. Wang, S. W., Gan, L., Martin, S. E. & Klein, W. H. Abnormal polarization and axon  
1058 outgrowth in retinal ganglion cells lacking the POU-domain transcription factor Brn-  
1059 3b. *Mol Cell Neurosci* **16**, 141–56 (2000).
- 1060 52. Ge, Y., Wu, F., Cheng, M., Bard, J. & Mu, X. Two new genetically modified mouse  
1061 alleles labeling distinct phases of retinal ganglion cell development by fluorescent  
1062 proteins. *Dev. Dyn. Off. Publ. Am. Assoc. Anat.* (2020) doi:10.1002/dvdy.233.
- 1063 53. Gan, L., Wang, S. W., Huang, Z. & Klein, W. H. POU domain factor Brn-3b is  
1064 essential for retinal ganglion cell differentiation and survival but not for initial cell  
1065 fate specification. *Dev Biol* **210**, 469–80 (1999).
- 1066 54. Dobin, A. *et al.* STAR: ultrafast universal RNA-seq aligner. *Bioinformatics* **29**, 15–  
1067 21 (2013).
- 1068 55. Robinson, M. D., McCarthy, D. J. & Smyth, G. K. edgeR: a Bioconductor package  
1069 for differential expression analysis of digital gene expression data. *Bioinformatics*  
1070 **26**, 139–40 (2010).

- 1071 56. Wu, F., Sapkota, D., Li, R. & Mu, X. Onecut 1 and Onecut 2 are potential regulators  
1072 of mouse retinal development. *J Comp Neurol* **520**, 952–69 (2012).
- 1073 57. Tirosh, I. *et al.* Dissecting the multicellular ecosystem of metastatic melanoma by  
1074 single-cell RNA-seq. *Science* **352**, 189–196 (2016).
- 1075 58. Haghverdi, L., Büttner, M., Wolf, F. A., Büttner, F. & Theis, F. J. Diffusion  
1076 pseudotime robustly reconstructs lineage branching. *Nat. Methods* **13**, 845–848  
1077 (2016).
- 1078 59. Wu, F. *et al.* Two transcription factors, Pou4f2 and Isl1, are sufficient to specify the  
1079 retinal ganglion cell fate. *Proc Natl Acad Sci U S A* **112**, E1559–68 (2015).
- 1080 60. Mu, X. *et al.* Discrete gene sets depend on POU domain transcription factor  
1081 Brn3b/Brn-3.2/POU4f2 for their expression in the mouse embryonic retina.  
1082 *Development* **131**, 1197–210 (2004).
- 1083 61. Qiu, F., Jiang, H. & Xiang, M. A comprehensive negative regulatory program  
1084 controlled by Brn3b to ensure ganglion cell specification from multipotential retinal  
1085 precursors. *J Neurosci* **28**, 3392–403 (2008).
- 1086 62. Huang, D. W., Sherman, B. T. & Lempicki, R. A. Bioinformatics enrichment tools:  
1087 paths toward the comprehensive functional analysis of large gene lists. *Nucleic  
1088 Acids Res.* **37**, 1–13 (2009).
- 1089 63. de Melo, J. *et al.* Dlx1 and Dlx2 function is necessary for terminal differentiation  
1090 and survival of late-born retinal ganglion cells in the developing mouse retina. *Dev.  
1091 Camb. Engl.* **132**, 311–322 (2005).
- 1092 64. Zhang, Q. *et al.* Regulation of Brn3b by DLX1 and DLX2 is required for retinal  
1093 ganglion cell differentiation in the vertebrate retina. *Dev. Camb. Engl.* **144**, 1698–  
1094 1711 (2017).
- 1095 65. Mu, X. *et al.* Ganglion cells are required for normal progenitor- cell proliferation but  
1096 not cell-fate determination or patterning in the developing mouse retina. *Curr Biol*  
1097 **15**, 525–30 (2005).
- 1098 66. Sakagami, K., Gan, L. & Yang, X.-J. Distinct effects of Hedgehog signaling on  
1099 neuronal fate specification and cell cycle progression in the embryonic mouse  
1100 retina. *J. Neurosci. Off. J. Soc. Neurosci.* **29**, 6932–6944 (2009).
- 1101 67. Wang, Y., Dakubo, G. D., Thurig, S., Mazerolle, C. J. & Wallace, V. A. Retinal  
1102 ganglion cell-derived sonic hedgehog locally controls proliferation and the timing of  
1103 RGC development in the embryonic mouse retina. *Development* **132**, 5103–13  
1104 (2005).
- 1105 68. Zhang, X. M. & Yang, X. J. Regulation of retinal ganglion cell production by Sonic  
1106 hedgehog. *Development* **128**, 943–57 (2001).
- 1107 69. Bosanac, I. *et al.* The structure of SHH in complex with HHIP reveals a recognition  
1108 role for the Shh pseudo active site in signaling. *Nat Struct Mol Biol* **16**, 691–7  
1109 (2009).
- 1110 70. Lee, R. T. H., Zhao, Z. & Ingham, P. W. Hedgehog signalling. *Development* **143**,  
1111 367–372 (2016).
- 1112 71. Varjosalo, M. & Taipale, J. Hedgehog: functions and mechanisms. *Genes Dev.* **22**,  
1113 2454–2472 (2008).
- 1114 72. Kim, J. *et al.* GDF11 controls the timing of progenitor cell competence in  
1115 developing retina. *Science* **308**, 1927–30 (2005).

- 1116 73. Hashimoto, T., Zhang, X. M., Chen, B. Y. & Yang, X. J. VEGF activates divergent  
1117 intracellular signaling components to regulate retinal progenitor cell proliferation  
1118 and neuronal differentiation. *Development* **133**, 2201–10 (2006).
- 1119 74. Wall, D. S. *et al.* Progenitor cell proliferation in the retina is dependent on Notch-  
1120 independent Sonic hedgehog/Hes1 activity. *J Cell Biol* **184**, 101–12 (2009).
- 1121 75. Stuart, T. *et al.* Comprehensive Integration of Single-Cell Data. *Cell* **177**, 1888-  
1122 1902.e21 (2019).
- 1123 76. Taranova, O. V. *et al.* SOX2 is a dose-dependent regulator of retinal neural  
1124 progenitor competence. *Genes Dev* **20**, 1187–202 (2006).
- 1125 77. Brown, N. L. *et al.* Math5 encodes a murine basic helix-loop-helix transcription  
1126 factor expressed during early stages of retinal neurogenesis. *Development* **125**,  
1127 4821–33 (1998).
- 1128 78. Xiang, M. *et al.* The Brn-3 family of POU-domain factors: primary structure, binding  
1129 specificity, and expression in subsets of retinal ganglion cells and somatosensory  
1130 neurons. *J Neurosci* **15**, 4762–85 (1995).
- 1131 79. Zhou, H., Yoshioka, T. & Nathans, J. Retina-derived POU-domain factor-1: a  
1132 complex POU-domain gene implicated in the development of retinal ganglion and  
1133 amacrine cells. *J Neurosci* **16**, 2261–74 (1996).
- 1134 80. Akagi, T. *et al.* Requirement of multiple basic helix-loop-helix genes for retinal  
1135 neuronal subtype specification. *J Biol Chem* **279**, 28492–8 (2004).
- 1136 81. Furukawa, T., Morrow, E. M. & Cepko, C. L. Crx, a novel otx-like homeobox gene,  
1137 shows photoreceptor-specific expression and regulates photoreceptor  
1138 differentiation. *Cell* **91**, 531–41 (1997).
- 1139 82. Calera, M. R. *et al.* Connexin43 is required for production of the aqueous humor in  
1140 the murine eye. *J. Cell Sci.* **119**, 4510–4519 (2006).
- 1141 83. Zhao, S., Chen, Q., Hung, F.-C. & Overbeek, P. A. BMP signaling is required for  
1142 development of the ciliary body. *Development* **129**, 4435–4442 (2002).
- 1143 84. Blackshaw, S. *et al.* Genomic analysis of mouse retinal development. *PLoS Biol* **2**,  
1144 E247 (2004).
- 1145 85. Green, E. S., Stubbs, J. L. & Levine, E. M. Genetic rescue of cell number in a  
1146 mouse model of microphthalmia: interactions between Chx10 and G1-phase cell  
1147 cycle regulators. *Development* **130**, 539–52 (2003).
- 1148 86. de Melo, J. *et al.* Lhx2 Is an Essential Factor for Retinal Gliogenesis and Notch  
1149 Signaling. *J Neurosci* **36**, 2391–405 (2016).
- 1150 87. Brzezinski, J. A. th, Uoon Park, K. & Reh, T. A. Blimp1 (Prdm1) prevents re-  
1151 specification of photoreceptors into retinal bipolar cells by restricting competence.  
1152 *Dev Biol* **384**, 194–204 (2013).
- 1153 88. Ng, L. *et al.* A thyroid hormone receptor that is required for the development of  
1154 green cone photoreceptors. *Nat Genet* **27**, 94–8 (2001).
- 1155 89. Rodgers, H. M., Belcastro, M., Sokolov, M. & Mathers, P. H. Embryonic markers of  
1156 cone differentiation. <http://www.molvis.org/molvis/v22/1455/> (2016).
- 1157 90. Trimarchi, J. M. *et al.* Molecular heterogeneity of developing retinal ganglion and  
1158 amacrine cells revealed through single cell gene expression profiling. *J Comp*  
1159 *Neurol* **502**, 1047–65 (2007).

- 1160 91. Bassett, E. A. *et al.* Overlapping expression patterns and redundant roles for AP-2  
1161 transcription factors in the developing mammalian retina. *Dev Dyn* **241**, 814–29  
1162 (2012).
- 1163 92. Goodson, N. B. *et al.* Prdm13 is required for Ebf3+ amacrine cell formation in the  
1164 retina. *Dev. Biol.* **434**, 149–163 (2018).
- 1165 93. Bélanger, M.-C., Robert, B. & Cayouette, M. Msx1-Positive Progenitors in the  
1166 Retinal Ciliary Margin Give Rise to Both Neural and Non-neural Progenies in  
1167 Mammals. *Dev. Cell* **40**, 137–150 (2017).
- 1168 94. Marcucci, F. *et al.* The Ciliary Margin Zone of the Mammalian Retina Generates  
1169 Retinal Ganglion Cells. *Cell Rep.* **17**, 3153–3164 (2016).
- 1170 95. Pennesi, M. E. *et al.* BETA2/NeuroD1 null mice: a new model for transcription  
1171 factor-dependent photoreceptor degeneration. *J Neurosci* **23**, 453–61 (2003).
- 1172 96. Diez-Roux, G. *et al.* A High-Resolution Anatomical Atlas of the Transcriptome in  
1173 the Mouse Embryo. *PLoS Biol.* **9**, (2011).
- 1174 97. Chang, K.-C. *et al.* Novel Regulatory Mechanisms for the SoxC Transcriptional  
1175 Network Required for Visual Pathway Development. *J. Neurosci. Off. J. Soc.*  
1176 *Neurosci.* **37**, 4967–4981 (2017).
- 1177 98. Jiang, Y. *et al.* Transcription factors SOX4 and SOX11 function redundantly to  
1178 regulate the development of mouse retinal ganglion cells. *J Biol Chem* **288**, 18429–  
1179 38 (2013).
- 1180 99. Kuwajima, T., Soares, C. A., Sitko, A. A., Lefebvre, V. & Mason, C. SoxC  
1181 Transcription Factors Promote Contralateral Retinal Ganglion Cell Differentiation  
1182 and Axon Guidance in the Mouse Visual System. *Neuron* **93**, 1110-1125.e5 (2017).
- 1183 100. Usui, A. *et al.* The early retinal progenitor-expressed gene Sox11 regulates the  
1184 timing of the differentiation of retinal cells. *Development* **140**, 740–750 (2013).
- 1185 101. Wang, F. *et al.* RNAscope: a novel in situ RNA analysis platform for formalin-fixed,  
1186 paraffin-embedded tissues. *J Mol Diagn* **14**, 22–9 (2012).
- 1187 102. Hufnagel, R. B., Le, T. T., Riesenber, A. L. & Brown, N. L. Neurog2 controls the  
1188 leading edge of neurogenesis in the mammalian retina. *Dev Biol* **340**, 490–503  
1189 (2010).
- 1190 103. Feng, L. *et al.* Requirement for Bhlhb5 in the specification of amacrine and cone  
1191 bipolar subtypes in mouse retina. *Development* **133**, 4815–25 (2006).
- 1192 104. Feng, L. *et al.* Brn-3b inhibits generation of amacrine cells by binding to and  
1193 negatively regulating DLX1/2 in developing retina. *Neuroscience* **195**, 9–20 (2011).
- 1194 105. Huang, L. *et al.* Bhlhb5 is required for the subtype development of retinal amacrine  
1195 and bipolar cells in mice. *Dev. Dyn. Off. Publ. Am. Assoc. Anat.* **243**, 279–289  
1196 (2014).
- 1197 106. Riesenber, A. N., Conley, K. W., Le, T. T. & Brown, N. L. Separate and coincident  
1198 expression of Hes1 and Hes5 in the developing mouse eye. *Dev. Dyn. Off. Publ.*  
1199 *Am. Assoc. Anat.* **247**, 212–221 (2018).
- 1200 107. Mao, B., Zhang, Z. & Wang, G. BTG2: A rising star of tumor suppressors (Review).  
1201 *Int. J. Oncol.* **46**, 459–464 (2015).
- 1202 108. Salvador, J. M., Brown-Clay, J. D. & Fornace, A. J. Gadd45 in stress signaling, cell  
1203 cycle control, and apoptosis. *Adv. Exp. Med. Biol.* **793**, 1–19 (2013).
- 1204 109. Tamura, R. E. *et al.* GADD45 proteins: central players in tumorigenesis. *Curr. Mol.*  
1205 *Med.* **12**, 634–651 (2012).



- 1206 110. Yuniati, L., Scheijen, B., van der Meer, L. T. & van Leeuwen, F. N. Tumor  
1207 suppressors BTG1 and BTG2: Beyond growth control. *J. Cell. Physiol.* **234**, 5379–  
1208 5389 (2019).
- 1209 111. Miesfeld, J. B., Glaser, T. & Brown, N. L. The dynamics of native Atoh7 protein  
1210 expression during mouse retinal histogenesis, revealed with a new antibody. *Gene*  
1211 *Expr. Patterns GEP* **27**, 114–121 (2018).
- 1212 112. Le, T. T., Wroblewski, E., Patel, S., Riesenber, A. N. & Brown, N. L. Math5 is  
1213 required for both early retinal neuron differentiation and cell cycle progression. *Dev*  
1214 *Biol* **295**, 764–78 (2006).
- 1215 113. Jadhav, A. P., Cho, S. H. & Cepko, C. L. Notch activity permits retinal cells to  
1216 progress through multiple progenitor states and acquire a stem cell property. *Proc*  
1217 *Natl Acad Sci U A* **103**, 18998–9003 (2006).
- 1218 114. Maurer, K. A., Riesenber, A. N. & Brown, N. L. Notch signaling differentially  
1219 regulates Atoh7 and Neurog2 in the distal mouse retina. *Development* **141**, 3243–  
1220 54 (2014).
- 1221 115. Perron, M. & Harris, W. A. Determination of vertebrate retinal progenitor cell fate by  
1222 the Notch pathway and basic helix-loop-helix transcription factors. *Cell Mol Life Sci*  
1223 **57**, 215–23 (2000).
- 1224 116. Riesenber, A. N. & Brown, N. L. Cell autonomous and nonautonomous  
1225 requirements for Deltalike1 during early mouse retinal neurogenesis. *Dev. Dyn. Off.*  
1226 *Publ. Am. Assoc. Anat.* **245**, 631–640 (2016).
- 1227 117. Riesenber, A. N., Liu, Z., Kopan, R. & Brown, N. L. Rbpj cell autonomous  
1228 regulation of retinal ganglion cell and cone photoreceptor fates in the mouse retina.  
1229 *J Neurosci* **29**, 12865–77 (2009).
- 1230 118. Yaron, O., Farhy, C., Marquardt, T., Applebury, M. & Ashery-Padan, R. Notch1  
1231 functions to suppress cone-photoreceptor fate specification in the developing  
1232 mouse retina. *Development* **133**, 1367–78 (2006).
- 1233 119. Furukawa, T., Mukherjee, S., Bao, Z. Z., Morrow, E. M. & Cepko, C. L. rax, Hes1,  
1234 and notch1 promote the formation of Muller glia by postnatal retinal progenitor cells.  
1235 *Neuron* **26**, 383–94 (2000).
- 1236 120. Lee, H. Y. *et al.* Multiple requirements for Hes 1 during early eye formation. *Dev*  
1237 *Biol* **284**, 464–78 (2005).
- 1238 121. Nelson, B. R., Gumuscu, B., Hartman, B. H. & Reh, T. A. Notch activity is  
1239 downregulated just prior to retinal ganglion cell differentiation. *Dev Neurosci* **28**,  
1240 128–41 (2006).
- 1241 122. Nelson, B. R., Hartman, B. H., Georgi, S. A., Lan, M. S. & Reh, T. A. Transient  
1242 inactivation of Notch signaling synchronizes differentiation of neural progenitor cells.  
1243 *Dev. Biol.* **304**, 479–498 (2007).
- 1244 123. Cau, E. & Blader, P. Notch activity in the nervous system: to switch or not switch?  
1245 *Neural Develop.* **4**, 36 (2009).
- 1246 124. Kageyama, R., Ohtsuka, T., Shimojo, H. & Imayoshi, I. Dynamic Notch signaling in  
1247 neural progenitor cells and a revised view of lateral inhibition. *Nat. Neurosci.* **11**,  
1248 1247–1251 (2008).
- 1249 125. Lathia, J. D., Mattson, M. P. & Cheng, A. Notch: From Neural Development to  
1250 Neurological Disorders. *J. Neurochem.* **107**, 1471–1481 (2008).

- 1251 126. Luo, H. *et al.* Forkhead box N4 (Foxn4) activates Dll4-Notch signaling to suppress  
1252 photoreceptor cell fates of early retinal progenitors. *Proc. Natl. Acad. Sci. U. S. A.*  
1253 **109**, E553-562 (2012).
- 1254 127. Nelson, B. R. *et al.* Acheate-scute like 1 (Ascl1) is required for normal delta-like (Dll)  
1255 gene expression and notch signaling during retinal development. *Dev. Dyn. Off.*  
1256 *Publ. Am. Assoc. Anat.* **238**, 2163–2178 (2009).
- 1257 128. Liu, W., Mo, Z. & Xiang, M. The Ath5 proneural genes function upstream of Brn3  
1258 POU domain transcription factor genes to promote retinal ganglion cell  
1259 development. *Proc Natl Acad Sci U A* **98**, 1649–54 (2001).
- 1260 129. Prasov, L., Nagy, M., Rudolph, D. D. & Glaser, T. Math5 (Atoh7) gene dosage  
1261 limits retinal ganglion cell genesis. *Neuroreport* **23**, 631–4 (2012).
- 1262 130. Zhang, X.-M., Hashimoto, T., Tang, R. & Yang, X.-J. Elevated expression of human  
1263 bHLH factor ATOH7 accelerates cell cycle progression of progenitors and  
1264 enhances production of avian retinal ganglion cells. *Sci. Rep.* **8**, 6823 (2018).
- 1265 131. Ali, F. *et al.* Cell cycle-regulated multi-site phosphorylation of Neurogenin 2  
1266 coordinates cell cycling with differentiation during neurogenesis. *Dev. Camb. Engl.*  
1267 **138**, 4267–4277 (2011).
- 1268 132. Moore, K. B., Schneider, M. L. & Vetter, M. L. Posttranslational mechanisms  
1269 control the timing of bHLH function and regulate retinal cell fate. *Neuron* **34**, 183–  
1270 195 (2002).
- 1271 133. Satou, Y. *et al.* Phosphorylation states change Otx2 activity for cell proliferation  
1272 and patterning in the *Xenopus* embryo. *Dev. Camb. Engl.* **145**, (2018).
- 1273 134. Tomic, G. *et al.* Phospho-regulation of ATOH1 Is Required for Plasticity of  
1274 Secretory Progenitors and Tissue Regeneration. *Cell Stem Cell* **23**, 436-443.e7  
1275 (2018).
- 1276 135. Brodie-Kommit, J. *et al.* Atoh7-independent specification of retinal ganglion cell  
1277 identity. *bioRxiv* 2020.05.27.116954 (2020) doi:10.1101/2020.05.27.116954.
- 1278 136. Mao, C. A., Wang, S. W., Pan, P. & Klein, W. H. Rewiring the retinal ganglion cell  
1279 gene regulatory network: Neurod1 promotes retinal ganglion cell fate in the  
1280 absence of Math5. *Development* **135**, 3379–88 (2008).

1281

1282

1283 **Figure legends:**

1284 **Figure 1.** Conventional RNA-seq identifies differentially expressed genes (DEGs) in  
1285 E14.5 *Atoh7*-null, *Pou4f2*-null, and *Isl1*-null retinas. **a.** Clustering of all DEGs across all  
1286 four genotypes based on Z scores indicates the *Atoh7*-null retina is least similar,  
1287 whereas the *Isl1*-null retina is most similar to the wild-type retina. The genes were  
1288 divided into five groups (1-5) based on how they are affected in the three mutants. **b.** A  
1289 Venn-diagram showing the overlaps of downregulated genes in all three mutant retinas.  
1290 **c.** A Venn-diagram showing the overlaps of upregulated genes in the three mutant  
1291 retinas.

1292 **Figure 2.** The Shh pathway is regulated by the RGC gene regulatory cascade at  
1293 multiple levels. **a.** Multiple component genes of the Shh pathway are downregulated in  
1294 the three mutant retinas. Error bars are standard deviation. P values between all  
1295 mutants and wild-type were all smaller than 0.001. **b.** A diagram showing how the  
1296 *Atoh7-Pou4f2/Isl1* gene regulatory cascade regulates the Shh pathway in the  
1297 developing retina in a complex manner, with multiple feedback loops.

1298 **Figure 3.** scRNA-seq analysis of E13.5 wild-type (WT) and *Atoh7*-null (MT) retinas. **a. b.**  
1299 As indicated, UMAP clustering leads to the same 11 overlapping clusters (C0-C10) with  
1300 both WT (**a**) and MT (**b**) retinal cells. **c.** Expression of known marker genes as  
1301 represented by a dot plot enables identity assignment of individual WT and MT clusters  
1302 (see text for details). As indicated, the sizes of the dots indicate the percentage of cells  
1303 expressing the gene in individual clusters and the color intensities denote average  
1304 expression levels. **d. e.** Cell cycle analysis determines the cell cycle status (G1, S, and  
1305 G2/M) of individual cells in the clusters. Note that largely the same cell cycle distribution  
1306 is observed in the WT (**d**) and MT (**e**) retinas, and that the cell cycle statuses correlate  
1307 with UMAP clustering.

1308 **Figure 4.** Cluster-specific gene expression reveals the relationships among the wild-  
1309 type clusters. **a.** A heatmap showing the top ten enriched genes in each cluster. Each  
1310 horizontal line represents one gene and each vertical line represents one cell. Data from  
1311 equal numbers (100) of cells from each cluster are shown. The heatmap demonstrates  
1312 the continuity and directionality between these clusters. **b.** A Venn diagram showing the  
1313 overlaps of enriched genes between naïve RPCs (nRPC, C0-C2), transitional RPCs  
1314 (tRPC, C3 and C4), and RGCs (C5 and C6). tRPCs have substantial overlaps with both  
1315 nRPCs and RGCs, but nRPCs and RGCs have very few overlapped genes, indicating  
1316 the unidirectional relationship of these clusters. **c. d.** Developmental trajectories  
1317 predicted by the SCANPY tool based on diffusion pseudotime (DPT). Three trajectories  
1318 representing the emergence of photoreceptors (PH), horizontal and amacrine cells  
1319 (H&A), and RGCs from RPCs are identified for both the wild-type (WT) (**c**) and *Atoh7*-  
1320 null (MT) (**d**) cells. Progression is color-coded and the direction of each lineage is  
1321 clearly discernible, although the RGC lineage of the MT cells does not advance as far  
1322 as the WT cells.

1323 **Figure 5.** Spatial expression of *Sox4* and *Sox11*. **a.** Feature plot heatmaps indicate that  
1324 both genes are expressed in all clusters but at much higher levels in differentiating cells,  
1325 and that their expression levels are comparable in wild-type (WT) and *Atoh7*-null (MT)  
1326 cells. **b.** Violin plots indicate that both genes are expressed in comparable levels in



1327 corresponding WT (red) and MT (blue) clusters. The heights of the plots represent  
1328 expression levels and the widths represent relative proportions of cells expressing the  
1329 gene at that level. **d. e.** In situ hybridization with RNAscope probes confirms that *Sox4*  
1330 and *Sox11* are expressed in both RPCs and RGCs. Note that both genes are highly  
1331 expressed in a subset of RPCs in the outside part of the retina, which presumably are  
1332 the transitional RPCs.

1333 **Figure 6.** Gene expression signature of transitional RPCs (C3, C4). **a.** Genes regulating  
1334 distinct lineages are expressed in a shared transitional state, namely transitional RPCs,  
1335 as demonstrated by a dot plot. Often these genes continue to be expressed in the  
1336 specific cell lineage they regulate, e.g. *Atoh7* and *Sox11* in RGCs (C5), and *Otx2* in  
1337 photoreceptors (C8, C9). **b.** Feature heatmap showing the expression of *Atoh7*,  
1338 *Neurod1*, and *Otx2* in the wild-type clusters. The dotted line demarcates the transitional  
1339 RPCs (C3 and C4). Consistent with the dot plot, all three genes are expressed in  
1340 transitional RPCs, but *Atoh7* is expressed in more transitional RPCs than *Neurod1* and  
1341 *Otx2*. Whereas *Atoh7* trails into all three lineages, *Neurod1* and *Otx2* only continue to  
1342 be expressed in photoreceptors. **c.** Percentage of cells expressing *Atoh7*, *Neurog2*,  
1343 *Neurod1*, and *Otx2* in the transitional RPCs (C3, C4) and nascent RGCs (C5) in the  
1344 wild-type (WT) and *Atoh7*-null (MT) retinas. **d.** Changes in activities of *Atoh7*, *Neurog2*,  
1345 *NeuroD1*, and *Otx2* as cells progress into distinct lineages. For each gene, the gene  
1346 activity in each cluster is derived by the expression level of that cluster divided by the  
1347 mean of all clusters. **e.** Additional genes, including many encoding components of the  
1348 Notch pathway, are enriched in the transitional RPCs (C3, C4). **f-h.**  
1349 Immunofluorescence staining shows substantial co-expression of *Atoh7* with *Olig2* (**f**),  
1350 *Otx2* (**g**), and *Foxn4* (**h**) in RPCs. Note the yellow cells are those expressing both  
1351 markers in each panel. In the case of *Otx2*, which is expressed in both RPCs and  
1352 photoreceptors (**g**), the co-expression only occurs in the RPCs.

1353 **Figure 7.** Comparison of wild-type and *Atoh7*-null clusters. **a.** Proportions of cells in  
1354 each wild-type (WT, red) and *Atoh7*-null (MT, blue) clusters. Nascent RGCs (C5) and  
1355 differentiated RGCs (C6) are highlighted by a red box. Note there is no major change in  
1356 the proportion of cells in C5, but a marked reduction in C6. **b.** Scatter plots comparing  
1357 gene expression in corresponding pairs of WT and MT clusters. The correlation  
1358 coefficients ( $R^2$ ) are shown for each pair. The C5 and C6 pairs have the lowest  $R^2$   
1359 values, indicating the most changes in gene expression. **c.** Violin plots showing cluster-  
1360 specific changes in expression of the Notch pathway genes. Note the distinct  
1361 expression patterns of individual genes and differential expression changes in the MT  
1362 clusters (see text for details).

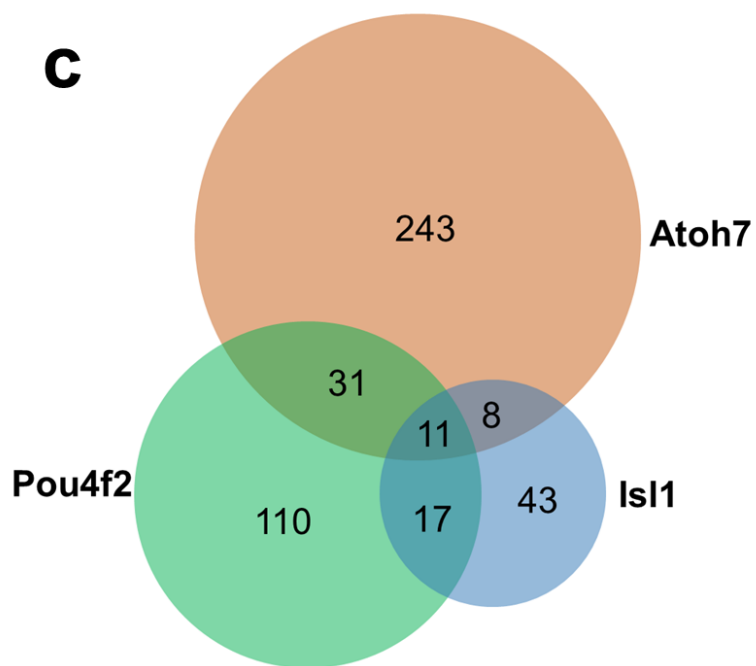
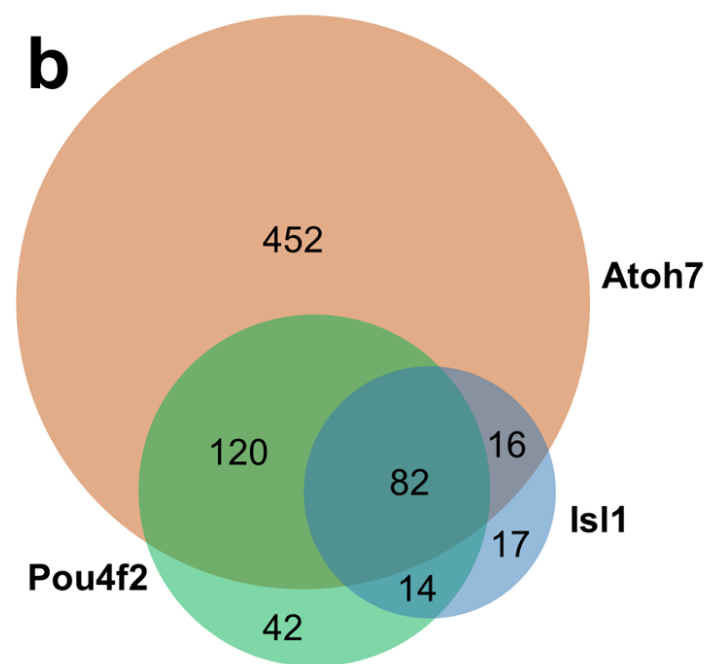
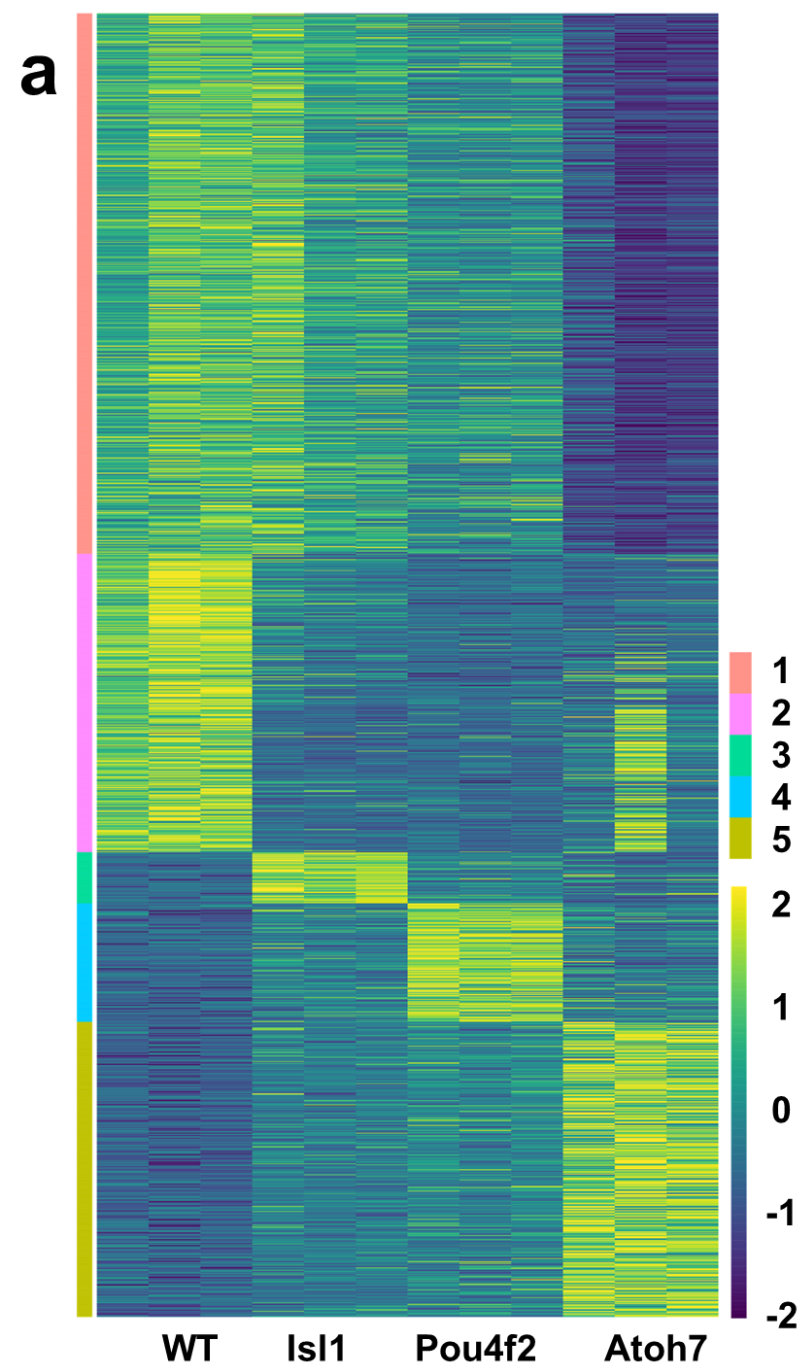
1363 **Figure 8.** Gene expression underlying the RGC lineage in the *Atoh7*-null retina. **a.**  
1364 Overlaps of down- and upregulated DEGs (DN and UP respectively) in *Atoh7*-null RGCs  
1365 and RGC-enriched genes (EN) as presented by a Venn diagram. **b.** Euclidean distance  
1366 clustering demonstrating seven different modes of changes in gene expression in  
1367 *Atoh7*-null retinal RGCs (C5 and C6, see main text for details). For comparison,  
1368 expression in C3 and C4 are also presented. **c.** Example genes with different modes of  
1369 expression as demonstrated by violin plots, showing their expression across all clusters  
1370 of wild-type (WT, red) and *Atoh7*-null (MT, blue) cells. *Pou4f2* is from group 1a in B,

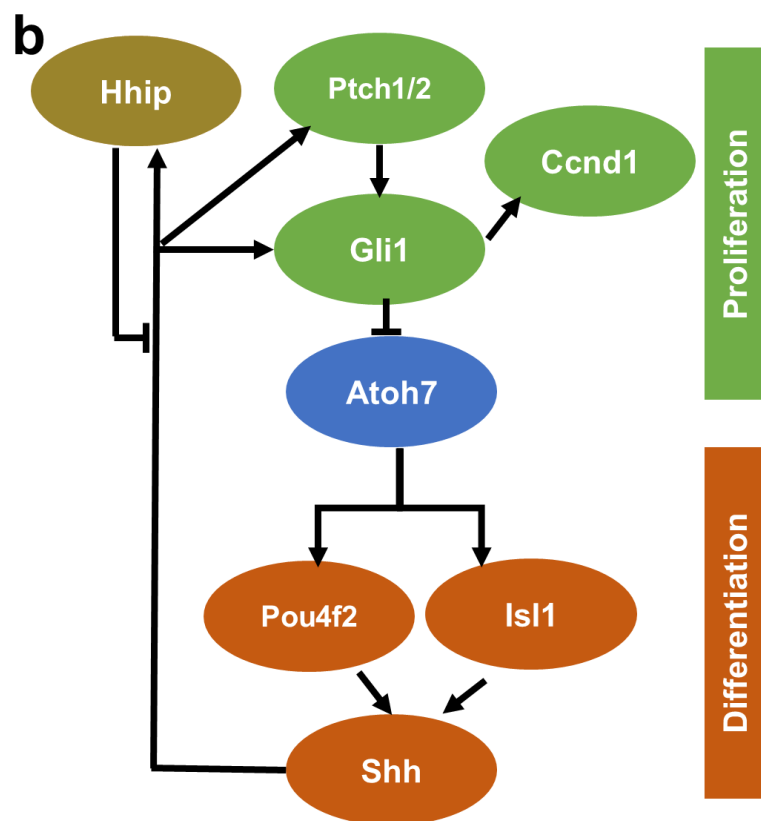
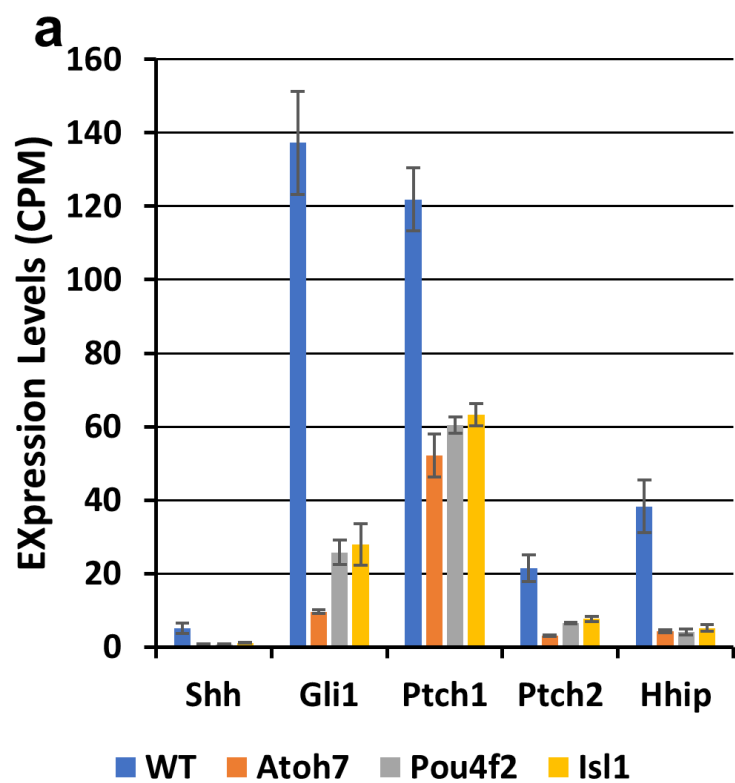
1371 *Syt4*, *Pou6f2*, *Gap43*, and *Elavl4* are from group 1b, *Nhlh2* is from group 2, *Kctd8* is  
1372 from group 3a, and *Neurod1* is from group 3b.

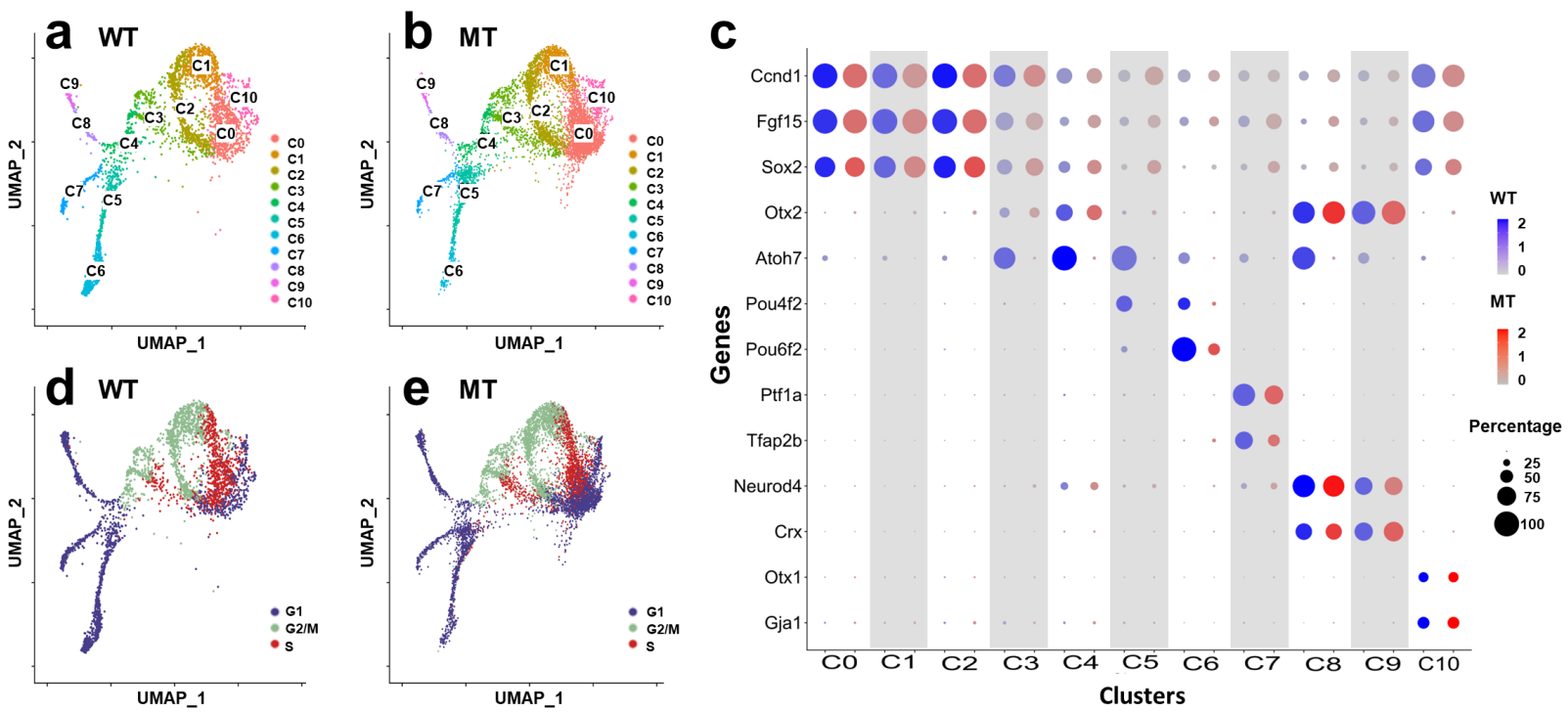
1373 **Figure 9.** Single cell RNA-seq analysis of E17.5 wild-type (WT) and *Atoh7*-null (MT)  
1374 cells. **a.** Identifies of UMAP clusters of WT and MT retinal cells, including naïve RPCs  
1375 (nRPC), transitional RPCs (tRPC), RGCs, horizontal and amacrine cells (H&A),  
1376 photoreceptors (PH). Note there are two transitional RPC clusters, two photoreceptor  
1377 clusters, and a cluster (?) whose identity needs to be further confirmed. **b.** Feature  
1378 heatmaps showing genes expressed in transitional RPCs, including *Atoh7*, *Neurog2*,  
1379 *Neurod1*, and *Otx2* in WT and MT retinas. **c.** Feature heatmaps of a set of RGC genes  
1380 in WT and MT retinas, including *Crabp1*, *Gal*, *Sncg*, and *Pou6f2*. *Crabp1*, *Gal*, and *Sncg*  
1381 are down-regulated, whereas *Pou6f2* is up-regulated, in the MT RGCs.

1382 **Figure 10.** A model explaining shifts of cell states along the RGC trajectory in the wild-  
1383 type and *Atoh7*-null retina. The RGC trajectory follows several four cell states, including  
1384 naïve RPCs, transitional RPCs, nascent RGCs, and differentiated RGCs. The direction  
1385 of the trajectory is indicated by the arrow and the progression of the trajectory is  
1386 indicated by a color gradient. Each state is determined by a group of genes and  
1387 example genes are given in colored circles. The transition from one state to the next is  
1388 dictated by downregulation of genes representing that state and upregulation of genes  
1389 for the next state as indicated by the sizes of the colored circles. In the transitional  
1390 RPCs, *Atoh7*, likely in combination with the SoxC factors, competes with other  
1391 regulators to drive them to the RGC fate. In the *Atoh7*-null retina, the establishment of  
1392 the transitional RPC state is not affected, and nascent RGCs still form through  
1393 expression of some, but not all, RGC genes (represented by a smaller circle with broken  
1394 lines). The mutant nascent RGCs fail to reach the full RGC state and many eventually  
1395 die by apoptosis (indicated by a striped background).

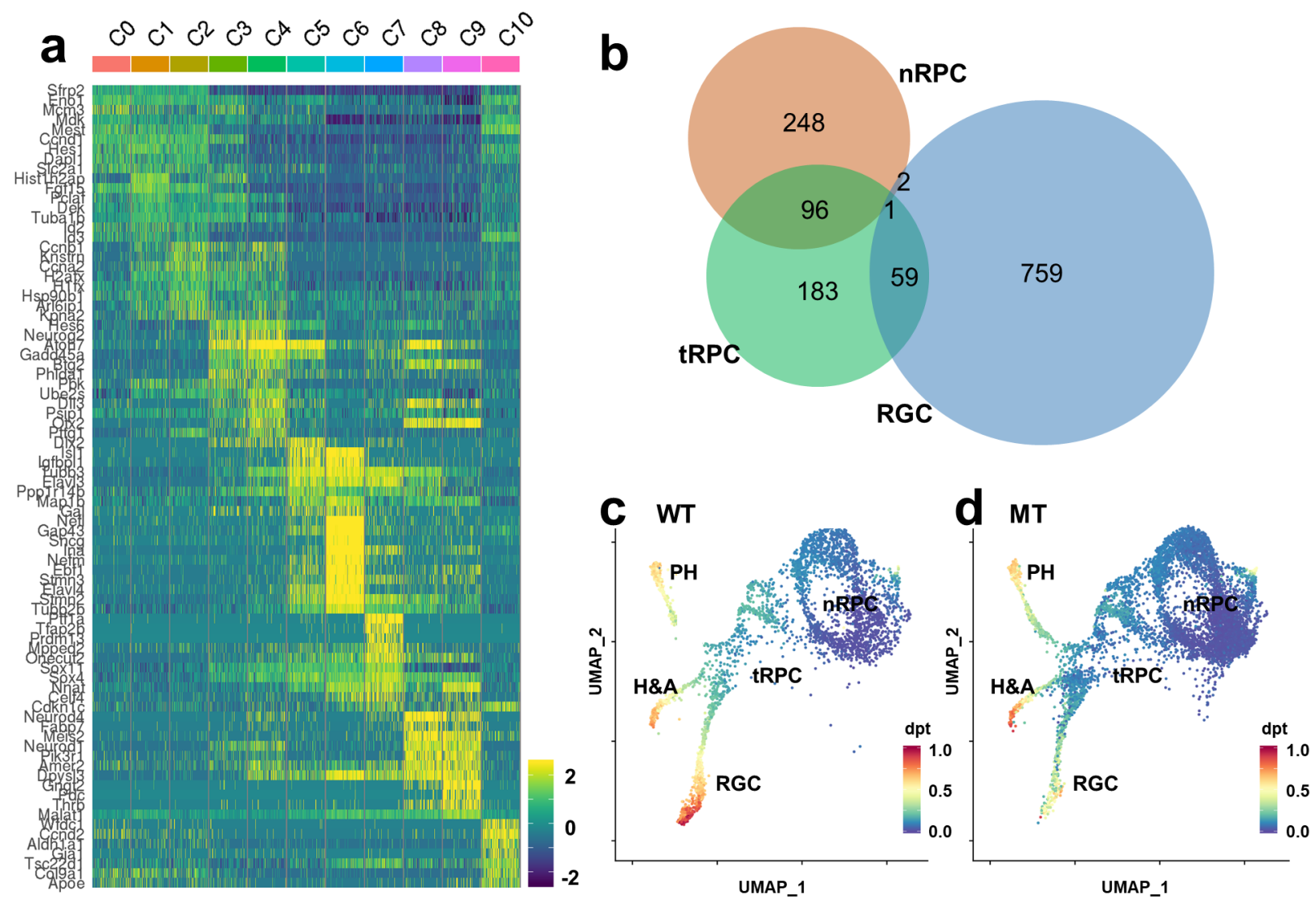
1396

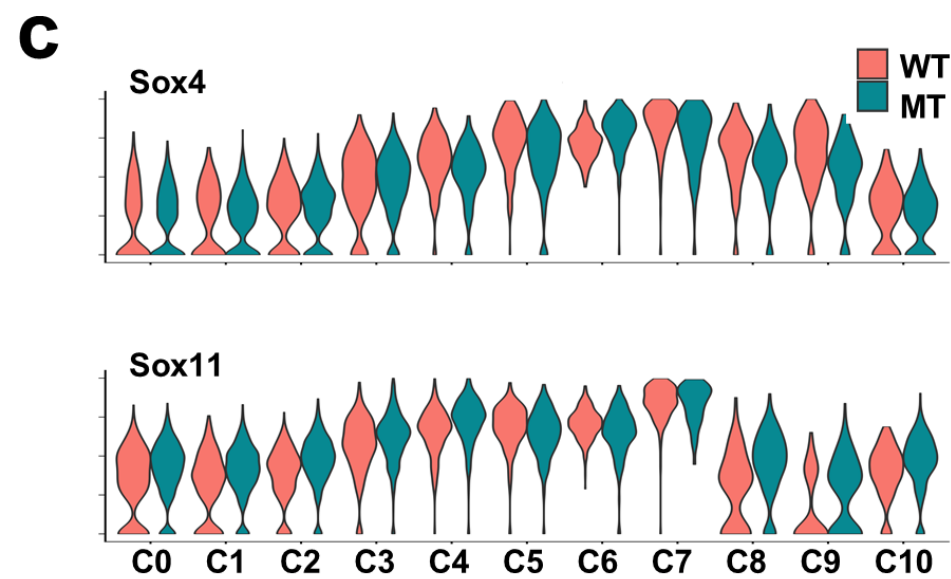
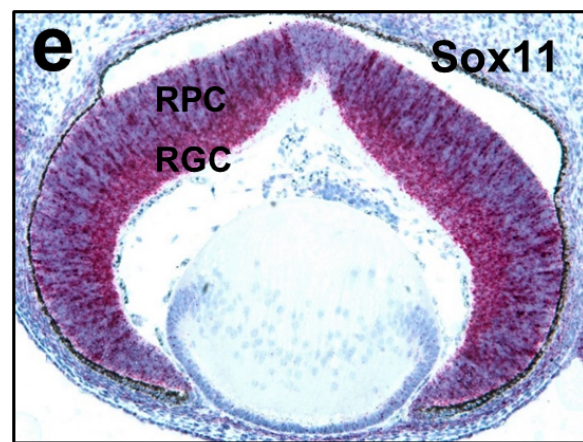
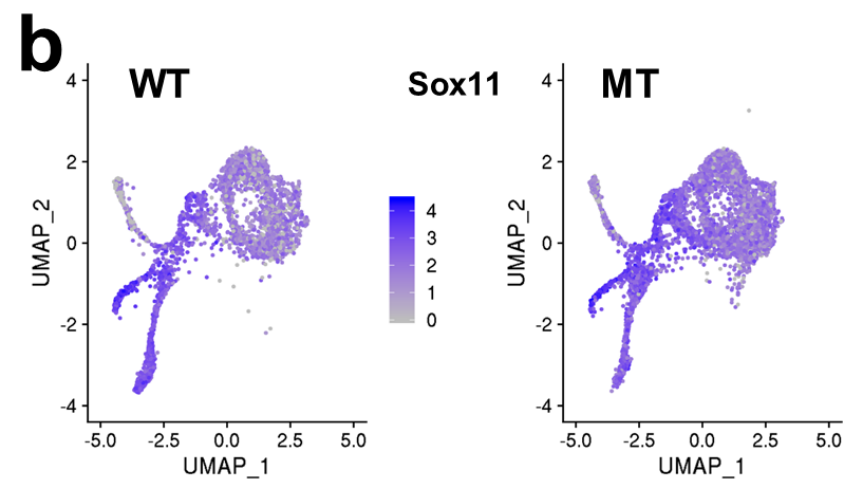
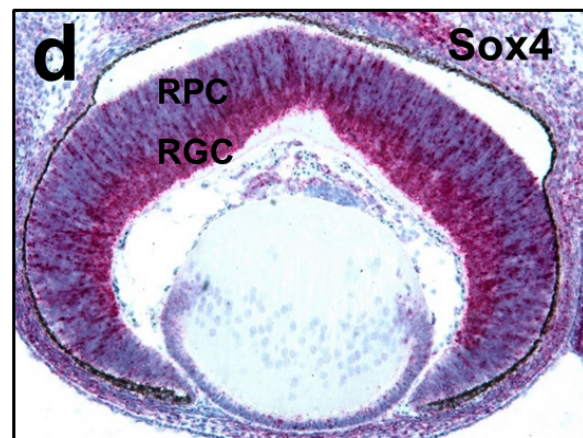
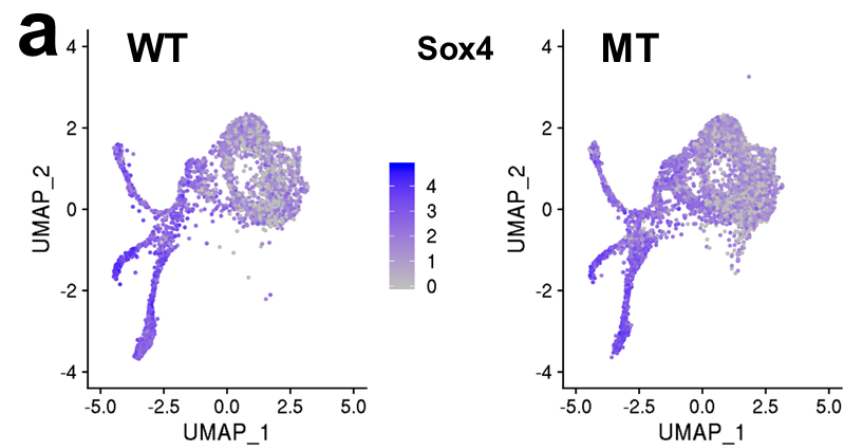


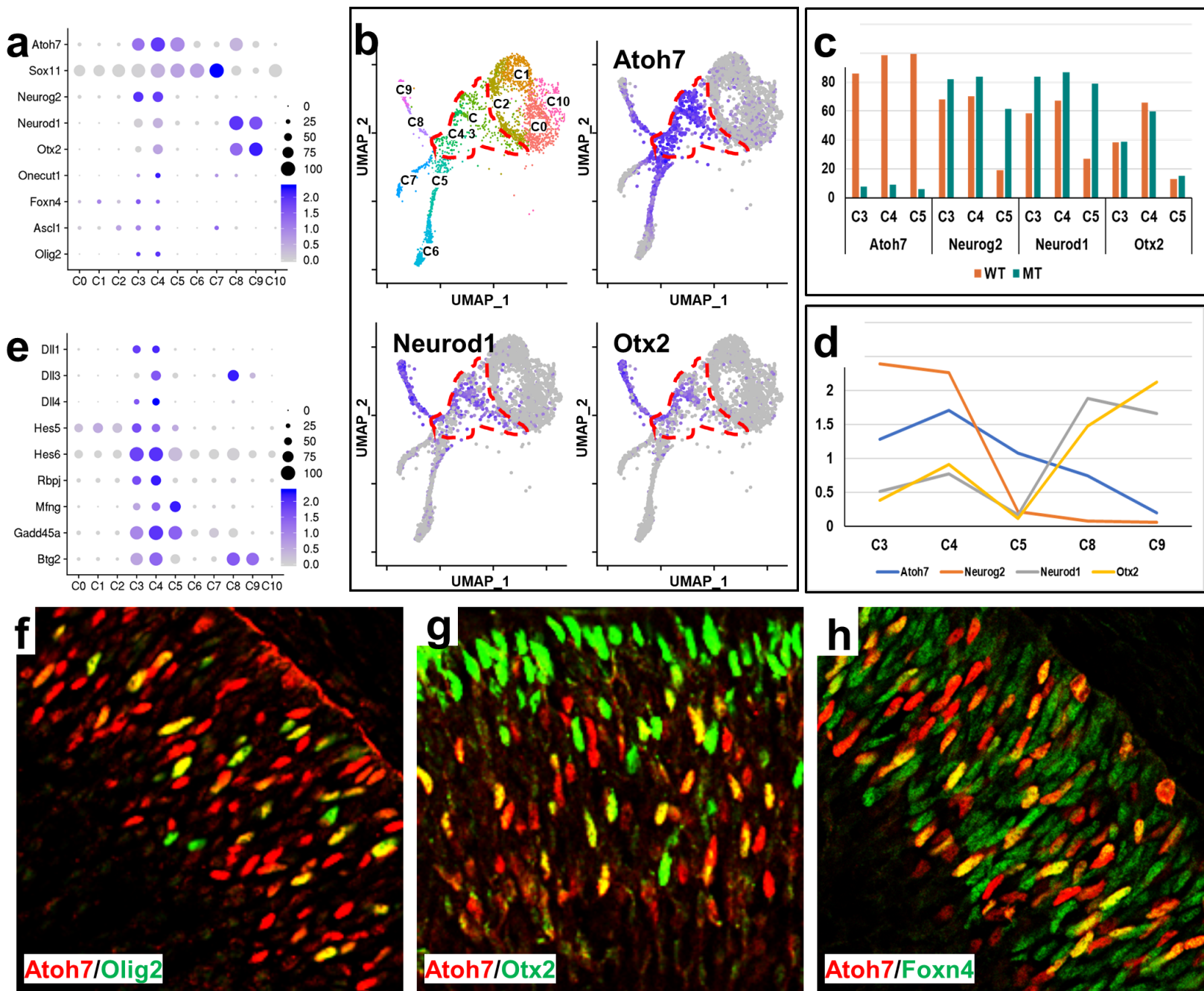


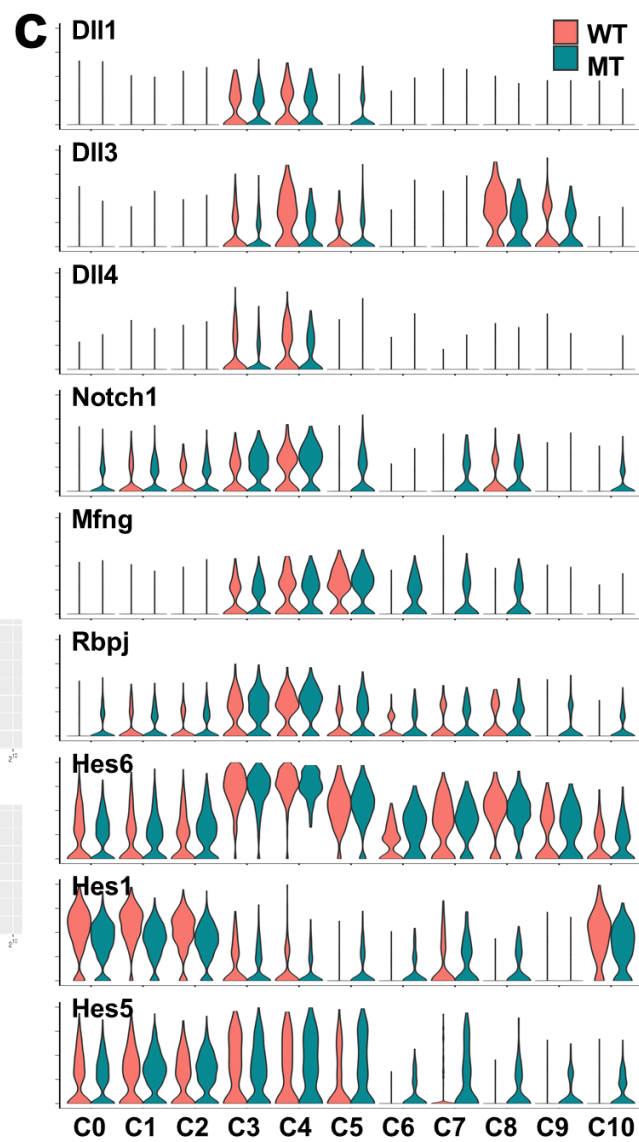
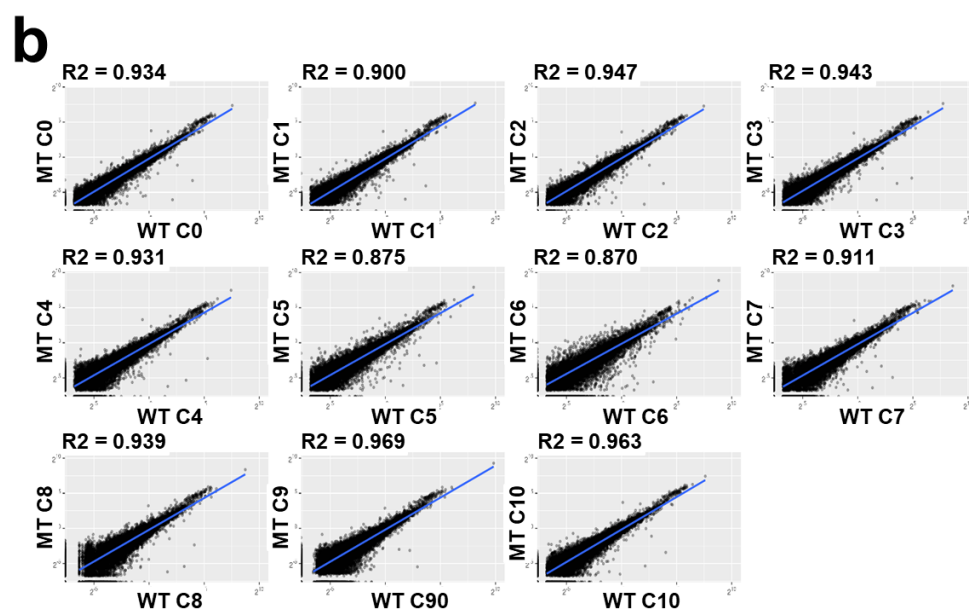
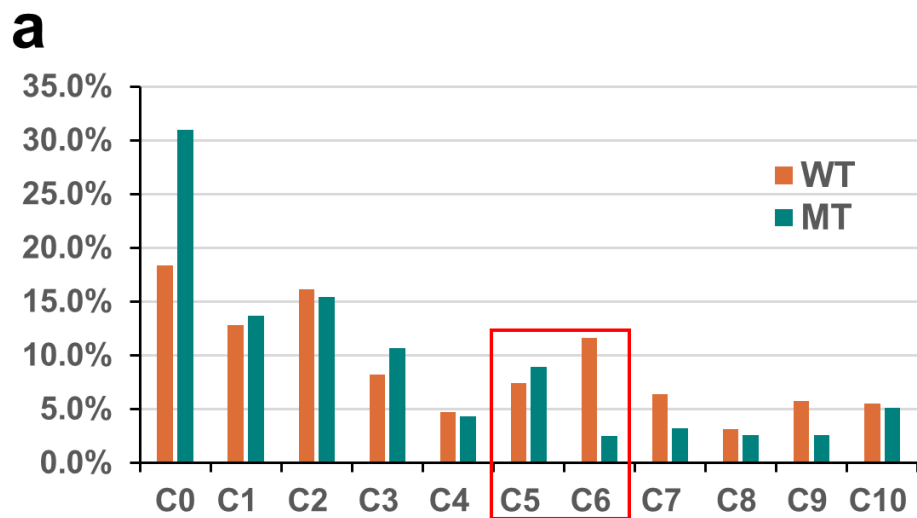




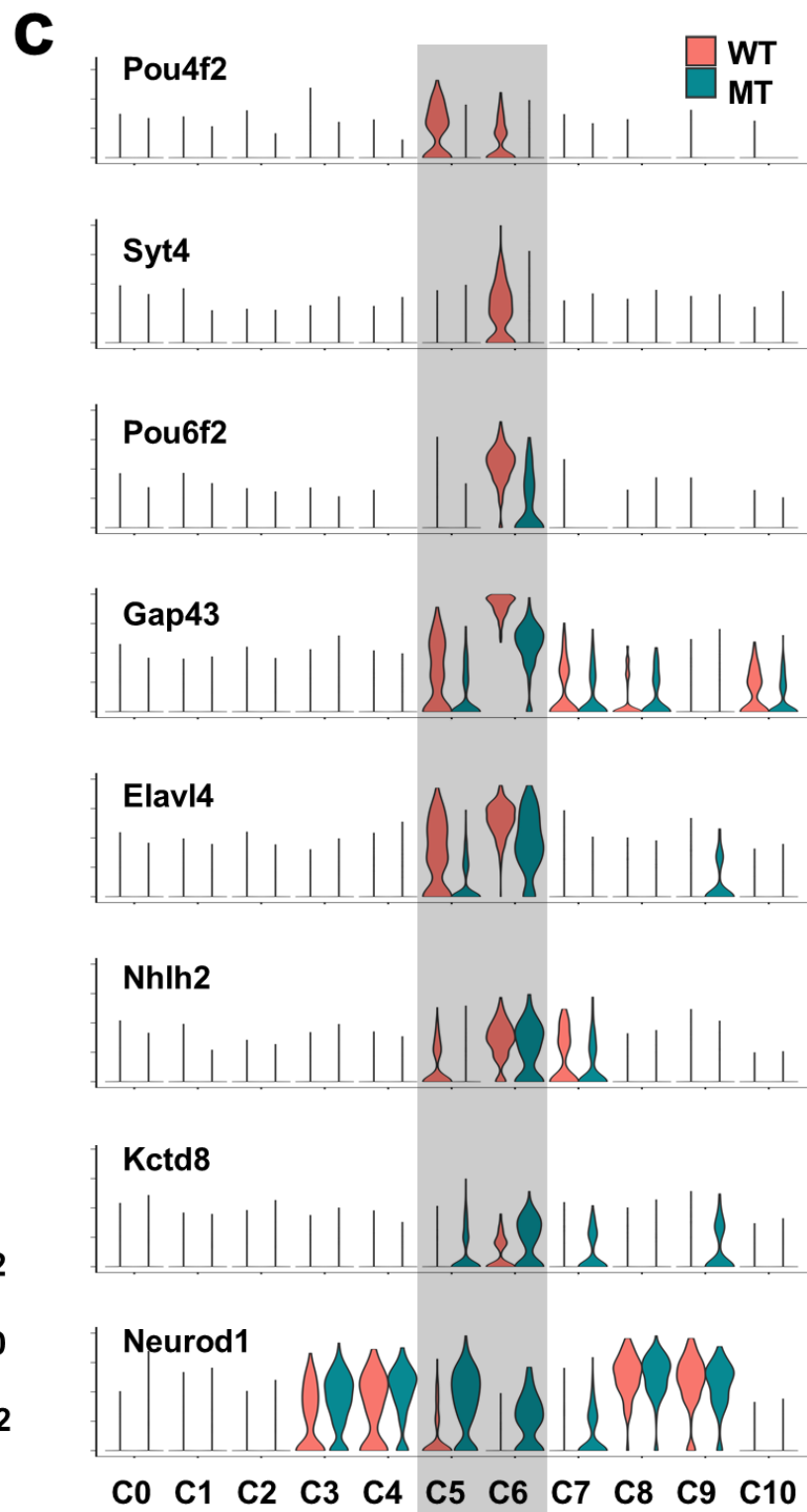
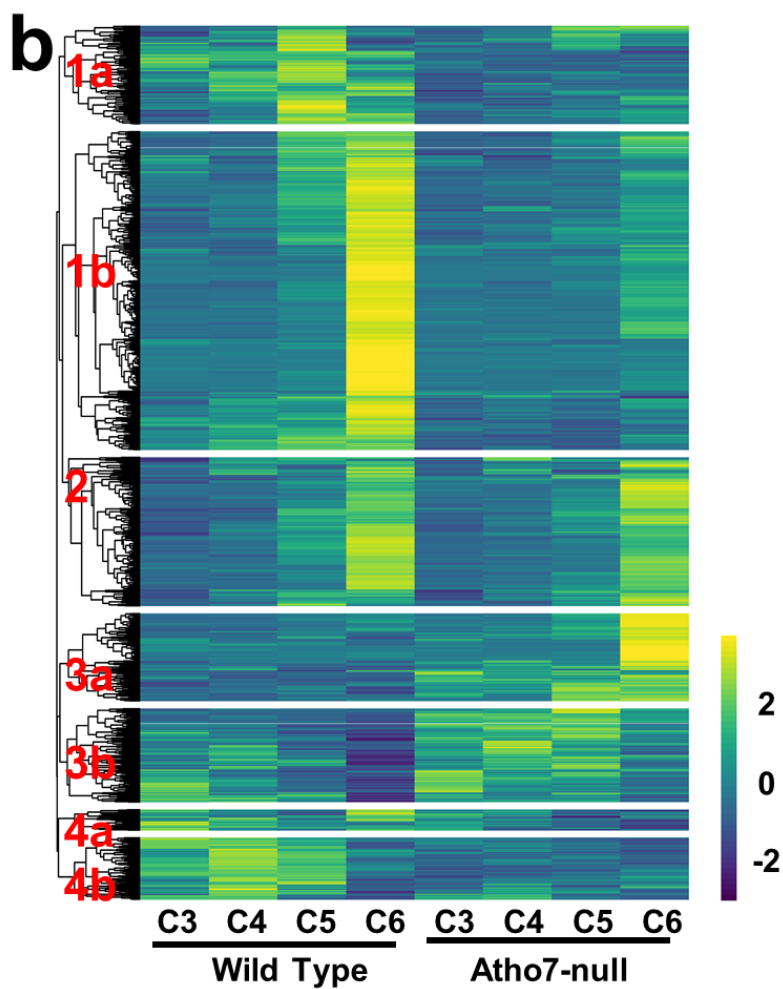
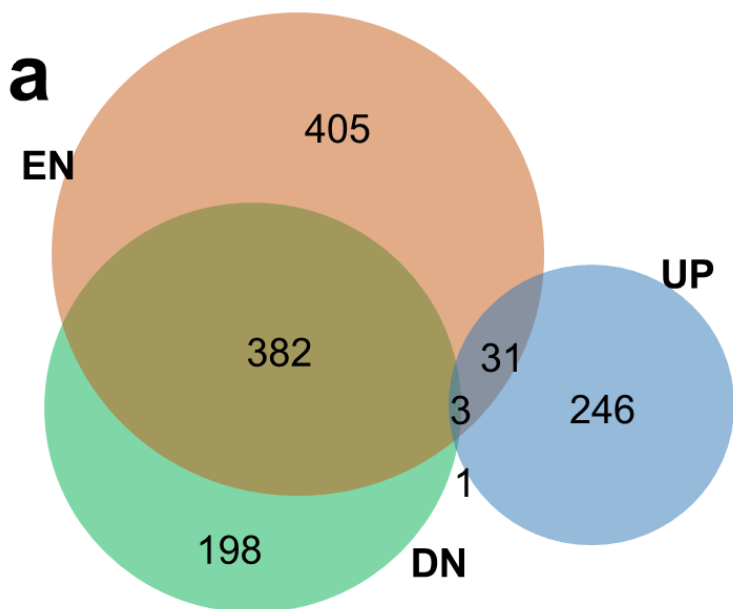




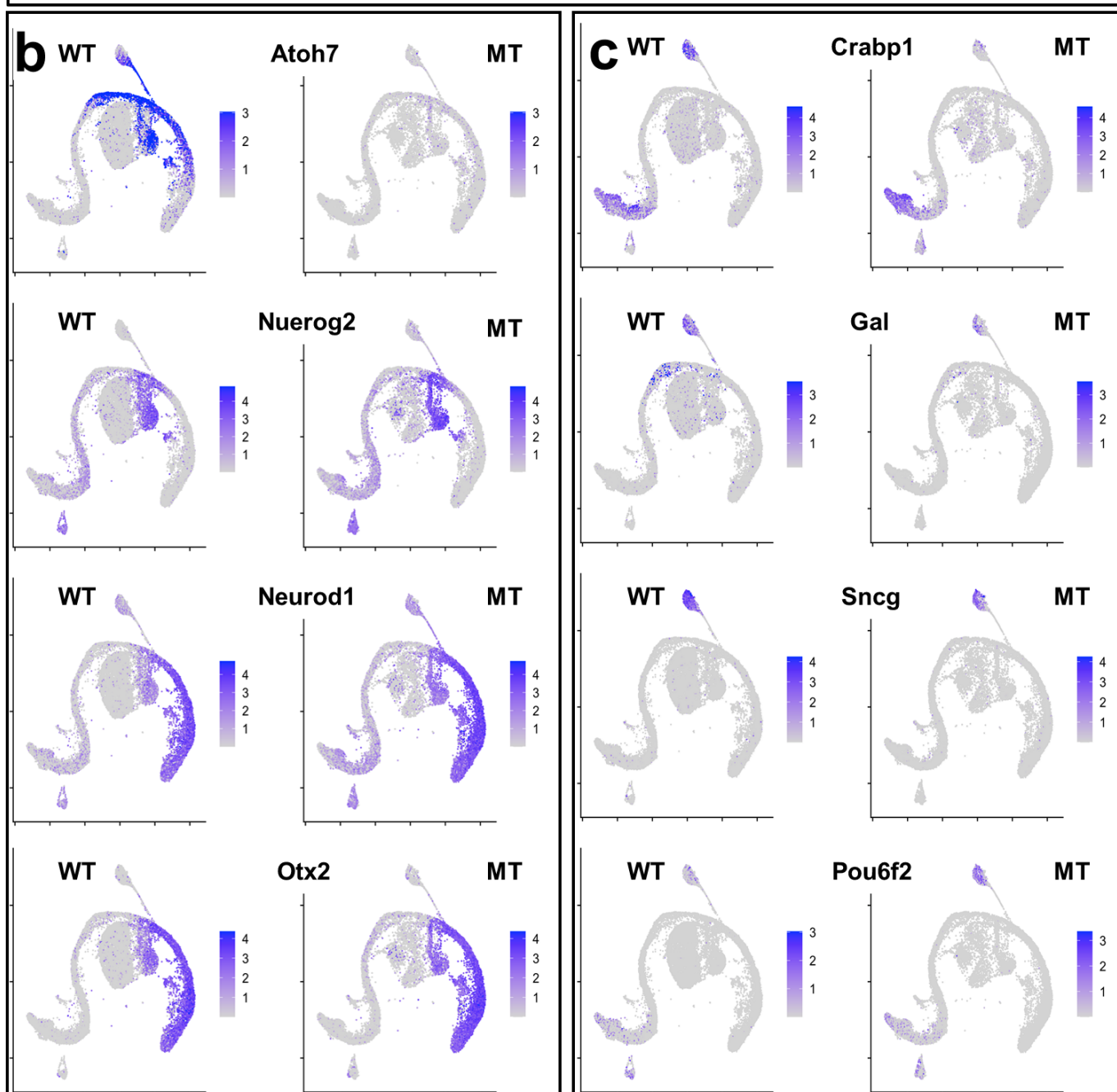
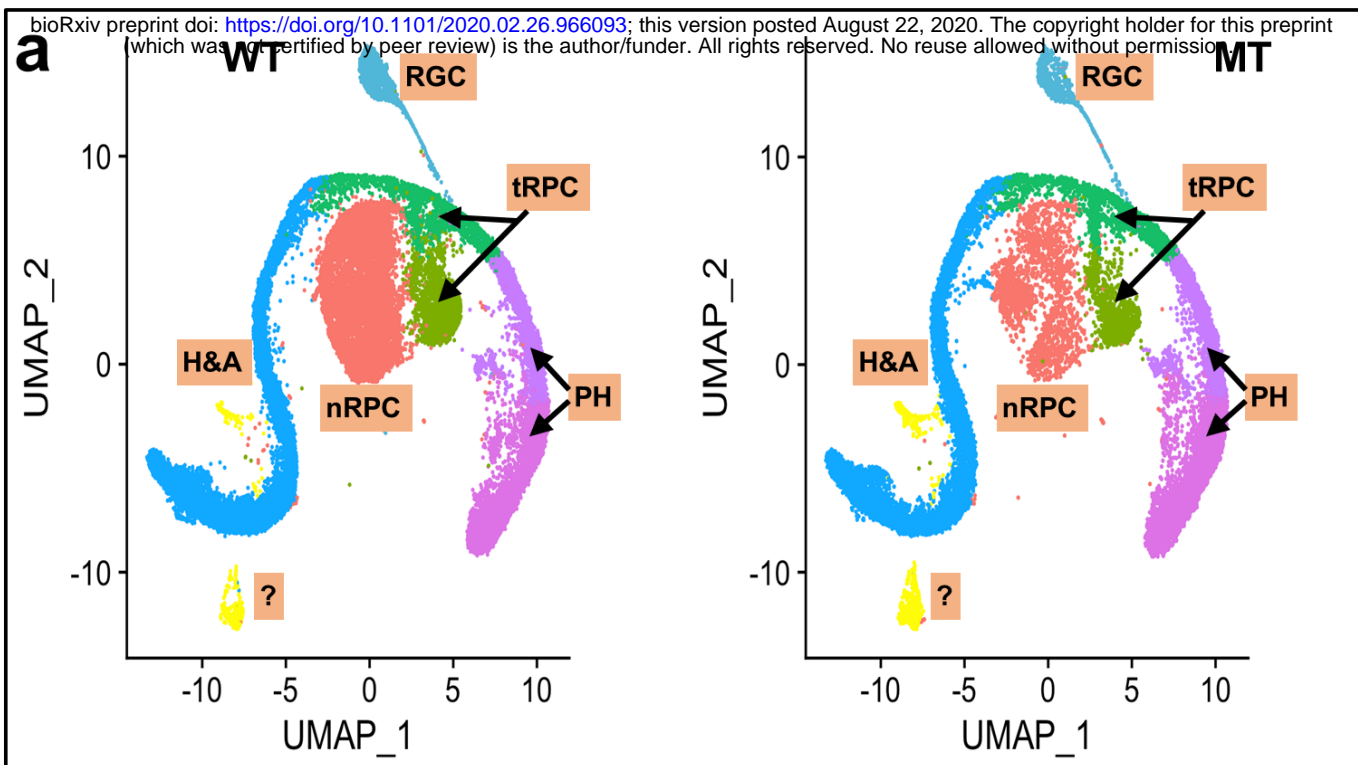












Progression of Cellular State

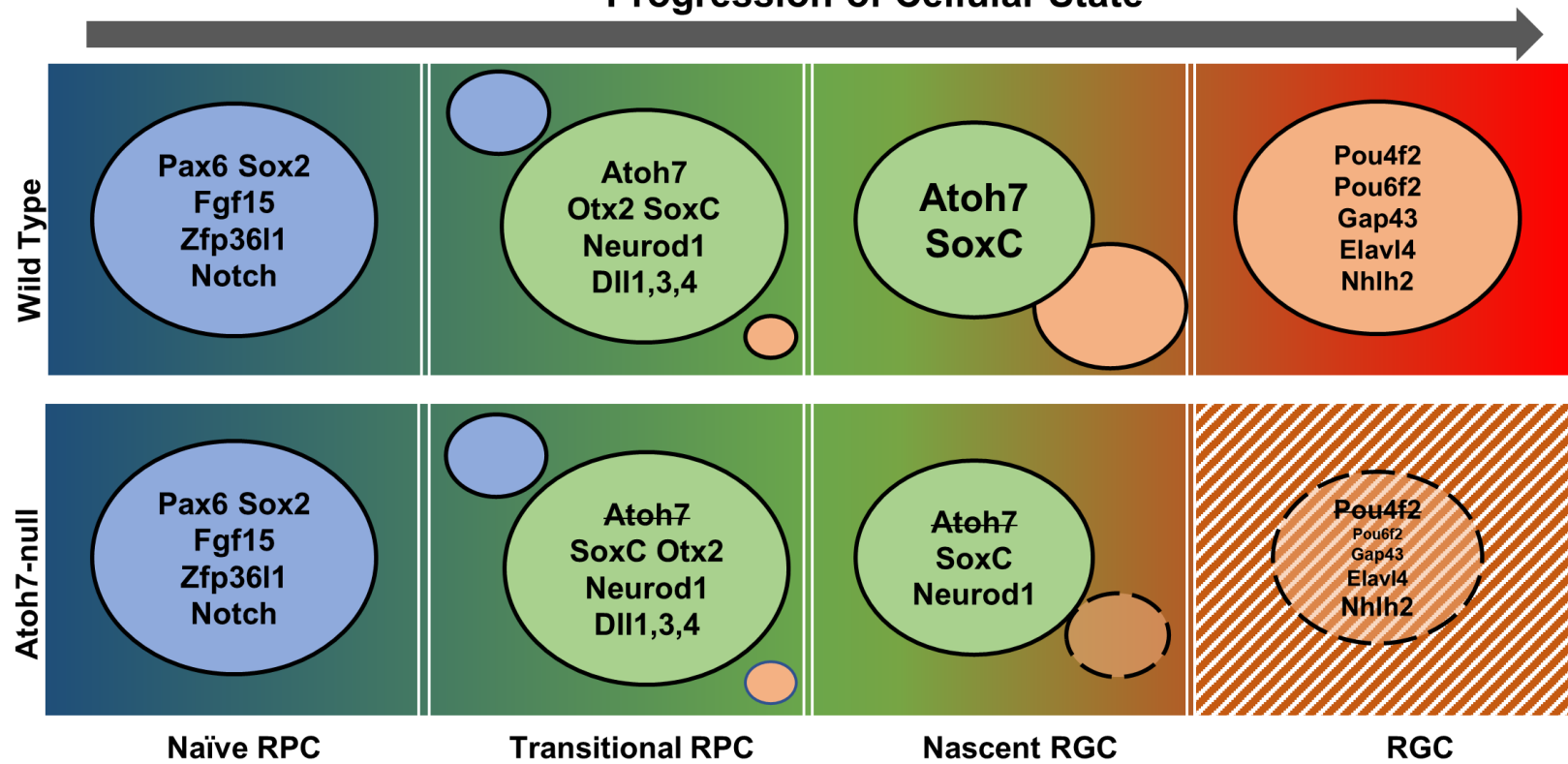


**Table 1. Enriched GO terms for individual cell states/types**

Term	Count	%	Fold Enrichment	P Value
<b>Naïve RPCs (C0-C3)</b>				
cell cycle	64	18.66	5.84	2.63E-30
cell division	51	14.87	7.63	2.13E-29
mitotic nuclear division	42	12.24	8.49	6.07E-26
nucleosome assembly	22	6.41	11.84	1.20E-16
chromosome segregation	16	4.66	10.06	4.83E-11
<b>Transitional RPCs (C3, C4)</b>				
RNA splicing	35	10.42	8.42	1.85E-21
cell cycle	51	15.18	4.81	2.52E-20
mRNA processing	37	11.01	6.66	3.06E-19
cell division	34	10.12	5.27	1.29E-14
mRNA splicing, via spliceosome	19	5.65	9.83	7.01E-13
<b>RGCs (C5, C6)</b>				
nervous system development	63	7.67	4.07	3.24E-21
axon guidance	31	3.78	5.07	3.39E-13
axonogenesis	25	3.05	5.69	7.00E-12
neuron projection development	24	2.92	4.21	1.07E-08
substantia nigra development	13	1.58	8.34	2.08E-08
<b>Photoreceptors (C8, C9)</b>				
nervous system development	30	8.17	4.35	7.13E-11
axon guidance	16	4.36	5.87	9.73E-08
cell differentiation	34	9.26	2.38	6.70E-06
neuron migration	12	3.27	5.29	1.71E-05
multicellular organism development	38	10.35	2.02	6.55E-05
<b>Amacrine and Horizontal Cells (C7)</b>				
visual perception	13	3.80	5.99	1.82E-06
photoreceptor cell maintenance	7	2.05	10.73	4.23E-05
synaptic vesicle exocytosis	5	1.46	16.13	2.19E-04
negative regulation of transcription from RNA polymerase II promoter	26	7.60	2.19	3.79E-04
positive regulation of transcription from RNA polymerase II promoter	32	9.36	1.97	4.08E-04

bioRxiv preprint doi: <https://doi.org/10.1101/2020.02.26.966093>; this version posted August 22, 2020. The copyright holder for this preprint (which was not certified by peer review) is the author/funder. All rights reserved. No reuse allowed without permission.

## Supplementary figure legends

**Supplementary Figure 1.** Feature plots demonstrating the cluster-specific expression of marker genes in both wild-type (WT) and *Atoh7*-null (MT) retinas at E13.5. These markers were used to assign identities to the clusters, including *Ccnd1* and *Fgf15* for naïve RPCs, *Atoh7* and *Otx2* for transitional RPCs, *Pou4f2* and *Pou6f2* for RGCs, *Ptf1a* and *Tfap2b* for amacrine and horizontal precursors, *Neurod4* and *Crx* for photoreceptors, and *Otx1* and *Gja1* for ciliary margin cells. Note that that expression of *Atoh7* and the two RGC marker genes *Pou4f2* and *Pou6f2* are diminished in the MT cells.

**Supplementary Figure 2.** Feature plots based on scRNA-seq showing the expression patterns of five naïve RPC enriched genes and ten RGC-enriched genes at E13.5. Comparing with in situ hybridization (see Suppl. Figure 3), scRNA-seq provides more details of cell type-specific expression. For example, *Fbxo5* is expressed only in subsets of naïve RPCs and transitional RPCs, which are likely in the late S and early G2/M phases of the cell cycle (compare with Figure 3d).

**Supplementary Figure 3.** In situ hybridization confirms the spatial expression patterns of five naïve RPC enriched genes and ten RGC-enriched genes. The in situ hybridization data were obtained from the Eurexpress database and match well with the enrichment results from our scRNA-seq analysis (See Suppl. Figure 2 and Suppl. Table 9).

**Supplementary Figure 4.** In situ hybridization with RNAscope probes confirms that *Gadd45a* and *Btg2* are expressed in subsets of RPCs with patterns similar to *Atoh7* in all three developmental stages (E12.5, E14.5, E16.5) examined.

**Supplementary Figure 5.** Feature plots of additional marker genes to identify clusters of the E17.5 scRNA-seq data. These markers include *Ccnd1* and *Sox2* for naïve RPCs, *Gadd45a* and *Btg2* for transitional RPCs, *Neurod4*, and *Crx* for photoreceptors, *Ptf1a* and *Tfab2b* for horizontal and amacrine cells, and *Pou4f2*, *Sst*, *Isl1*, and *Ebf1* for RGCs. WT is wild-type and MT is *Atoh7*-null.

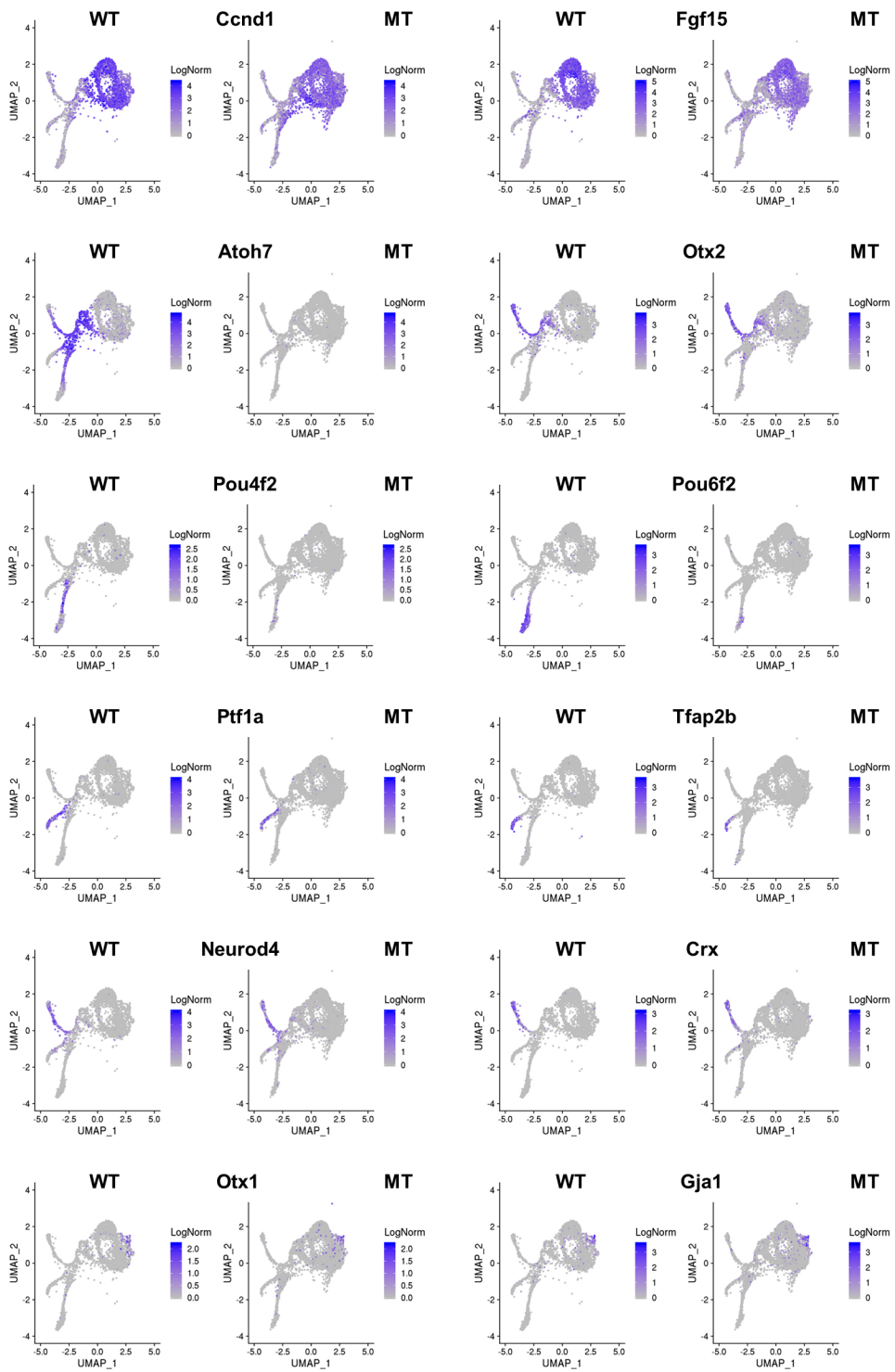
**Supplementary Figure 6.** Immunofluorescence staining for two RGC markers reveals that some RGCs persist in the *Atoh7*-null retina at E17.5. **a. b.** Expression of neurofilament middle chain (Nefm) in wild-type (WT) and *Atoh7*-null (MT) retinas. **c. d.** Expression of ubiquitin carboxy-terminal hydrolase L1 (Uchl1) in WT and MT retinas. Red is counterstaining by propidium iodide.

## List of Supplementary tables

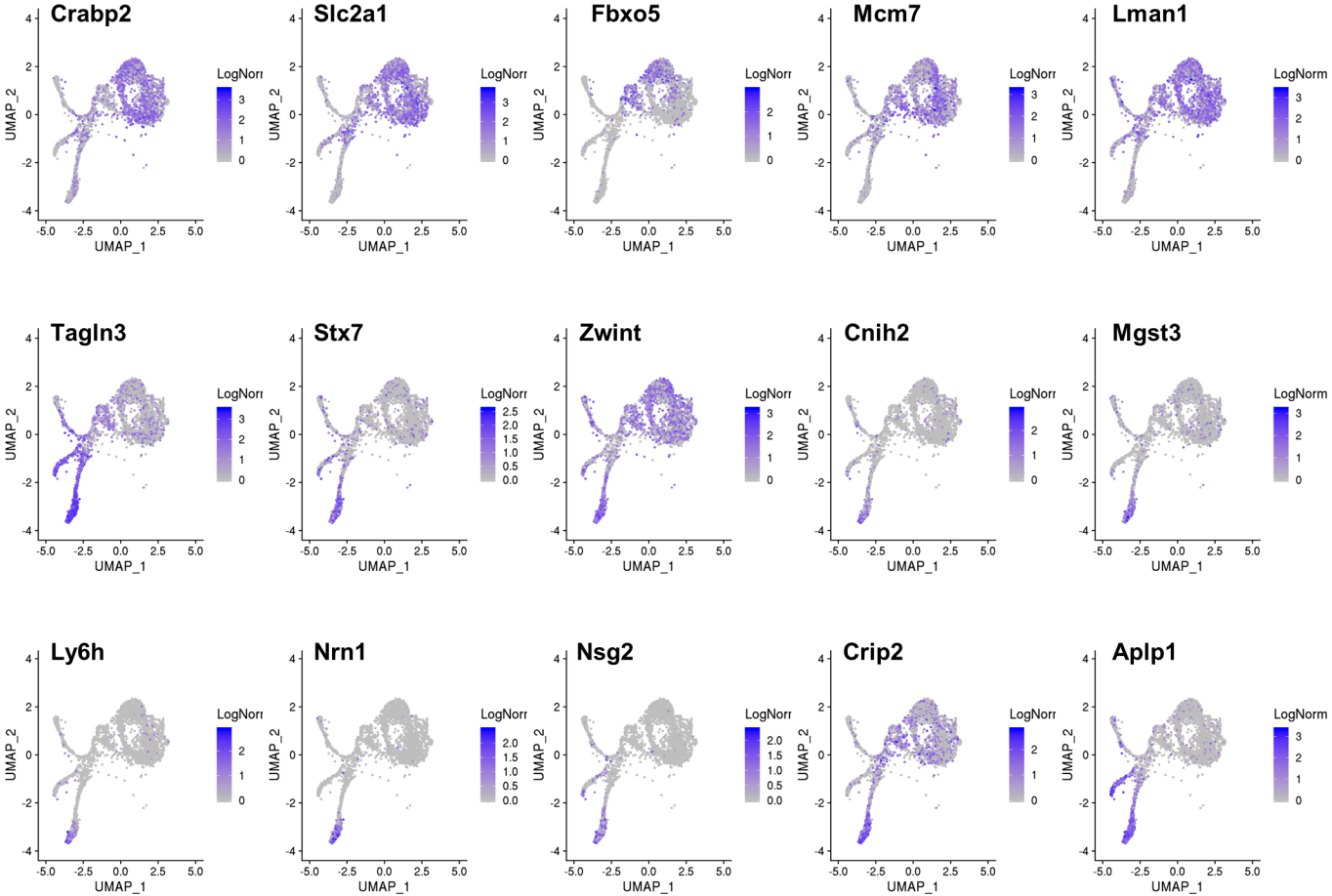
- Supplementary Table 1. All genes expressed in E14.5 wild-type retina
- Supplementary Table 2. Differentially expressed genes in E14.5 *Atoh7*-null retina
- Supplementary Table 3. Differentially expressed genes in E14.5 *Pou4f2*-null retina
- Supplementary Table 4. Differentially expressed genes in E14.5 *Isl1*-null retina
- Supplementary Table 5. Gene ontology analysis by DAVID of DEGs in E14.5 *Atoh7*-, *Pou4f2*-, and *Isl1*-null retinas
- Supplementary Table 6. Genes enriched in individual wild-type clusters
- Supplementary Table 7. Stats of cluster-enriched genes
- Supplementary Table 8. DEGs in C0 (270 genes)
- Supplementary Table 9. DEGs in C1 (203 genes)
- Supplementary Table 10. DEGs in C2 (216 genes)
- Supplementary Table 11. DEGs in C3 (229 genes)
- Supplementary Table 12. DEGs in C4 (128 genes)
- Supplementary Table 13. DEGs in C5 (450 genes)
- Supplementary Table 14. DEGs in C6 (618 genes)
- Supplementary Table 15. DEGs in C7 (114 genes)
- Supplementary Table 16. DEGs in C8 (58 genes)
- Supplementary Table 17. DEGs in C9 (55 genes)
- Supplementary Table 18. DEGs in C10 (94 genes)
- Supplementary Table 19. Gene Ontology analysis of DEGs in naïve RPCs, transitional RPCs, and RGCs
- Supplementary Table 20. Groups of C5/6 DEGs and enriched genes by K-means clustering
- Supplementary Table 21. DEGs in E17.5 naïve *Atoh7*-null RPCs
- Supplementary Table 22. DEGs in E17.5 transitional *Atoh7*-null RPCs (1)
- Supplementary Table 23. DEGs in E17.5 transitional *Atoh7*-null RPCs (2)
- Supplementary Table 24. DEGs in E17.5 *Atoh7*-null RGCs



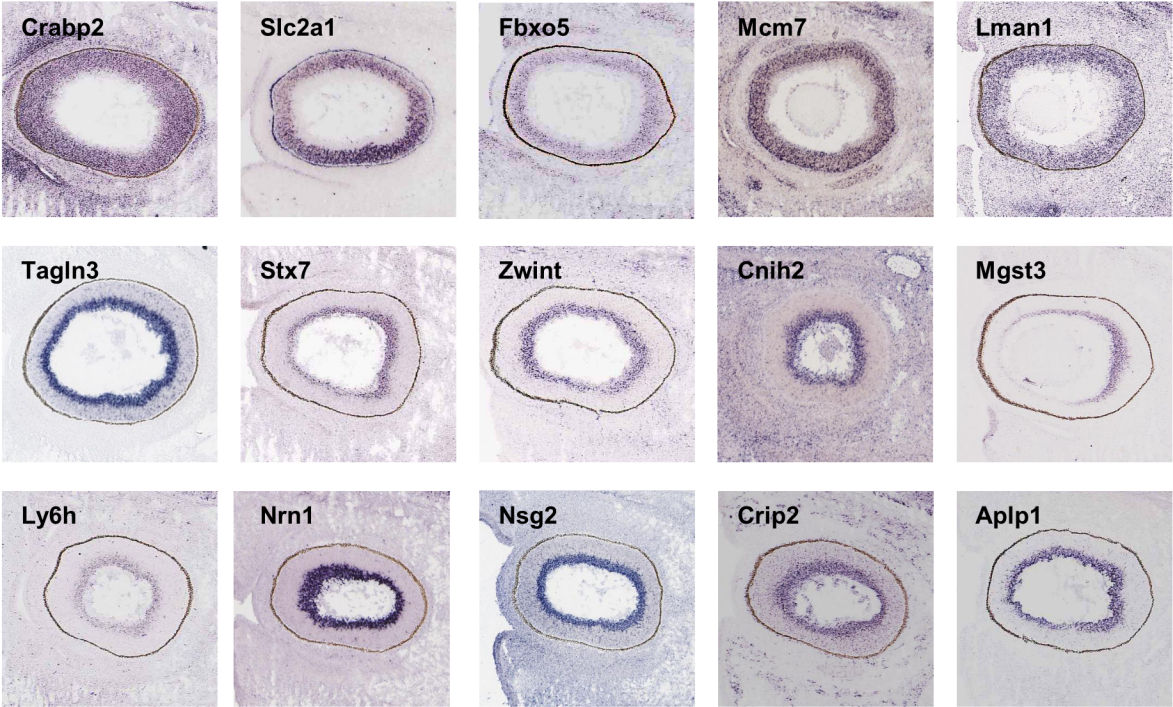
# Suppl. Figure 1



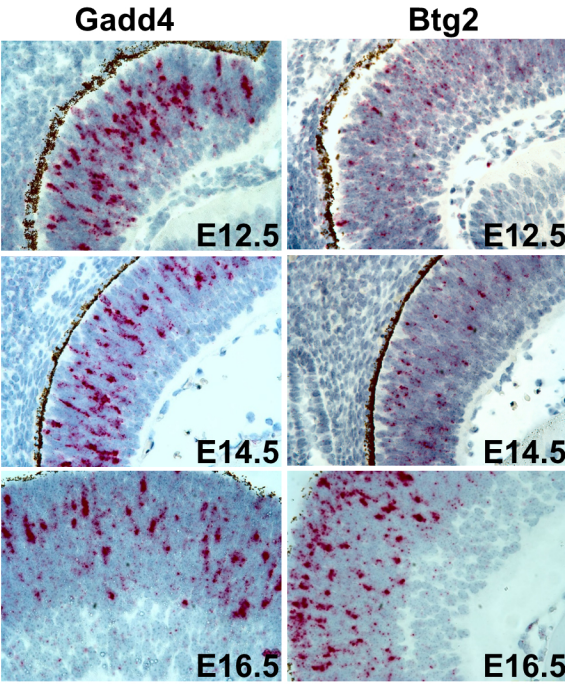
# Suppl. Figure 2



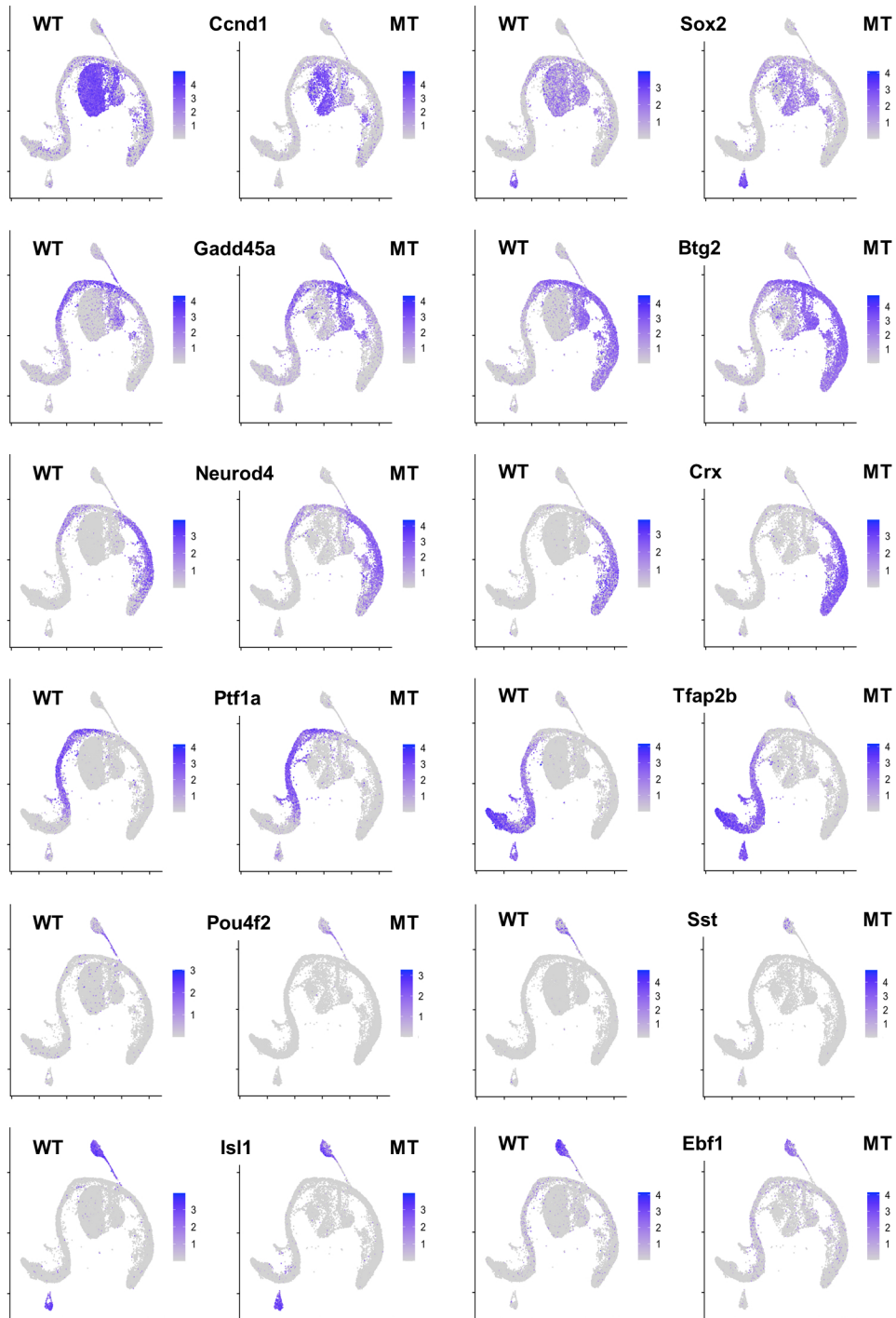
**Suppl. Figure 3**



**Suppl. Figure 4**



# Suppl. Figure 5





Suppl. Figure 6

